Jet substructure measurements with CMS

Kaustuv Datta (ETH Zürich)

on behalf of the CMS Collaboration

July 30, BOOST 2024

Outline

1. Introduction

2. Jet substructure measurements at CMS:

   a. *Measurement of the primary Lund jet plane density in proton-proton collisions at $\sqrt{s} = 13$ TeV*; JHEP 05 (2024) 116

   b. *Measurement of energy correlators inside jets and determination of the strong coupling $\alpha_S(m_Z)$*; arXiv:2402.13864

   c. *Girth and groomed radius of jets recoiling against isolated photons in lead-lead and proton-proton collisions at $\sqrt{s_{NN}} = 5.02$ TeV*; arXiv:2405.02737 (see Bharadwaj's talk)

   d. *Unfolding the jet axis decorrelation in pp and PbPb collisions at $\sqrt{s_{NN}} = 5.02$ TeV with CMS*; CERN-CMS-NOTE-2024-004 (see Molly's talk)

   e. *Jet fragmentation function and groomed substructure of bottom quark jets in proton-proton collisions at $\sqrt{s} = 5.02$ TeV*; CMS-PAS-HIN-24-005 (see Lida's talk)

   f. *Exploring small-angle emissions in D-tagged jets in proton-proton collisions at $\sqrt{s} = 5.02$ TeV*; CMS-PAS-HIN-24-007 (see Jelena's talk)

3. Summary

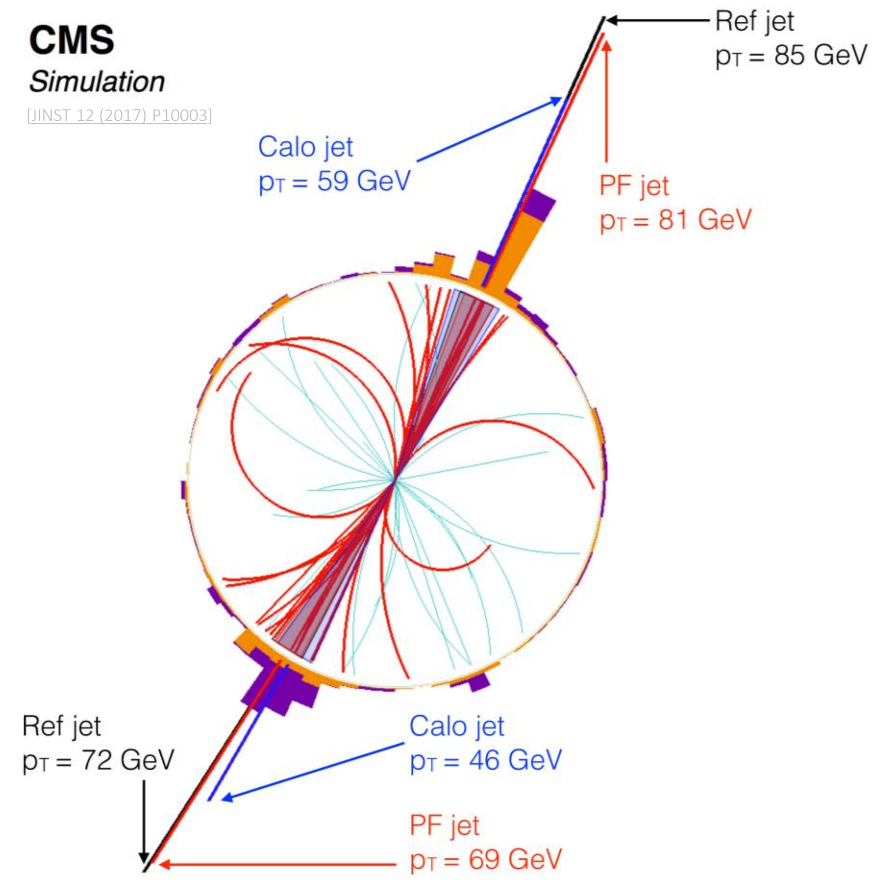

Introduction

(some) recent CMS measurements

- Jet substructure measurements a critical part of experimental programmes at LHC collaborations and beyond

  → experimental precision sufficient to compare unfolded measurements to state-of-the-art in analytic calculations in perturbative QCD

  → isolate modelling of different perturbative and non-perturbative contributions in a well-defined way

  → probe stages of jet formation, scaling properties of QCD

  → provide numerous handles for tuning Monte Carlo event generators, parton shower and hadronization models, custom underlying event tunes

  → reduction in uncertainties on other measurements/searches/ML taggers relying on accurate modelling of jet substructure

Reference, $\sqrt{s}$	Final state	Jets flavours, p_T (GeV)	Observables
1808.0734 13 TeV pp	$t\bar{t}$	q/g-jets (AK4), p_T>30 g-jets (AK4), p_T>30 b-jets (AK4), p_T>30	Jet substructure and softdrop observables
1809.08602 5.02 TeV pp/PbPb	jets	q/g-jets (AK3), p_T>30	Jet shapes
1911.038 13 TeV pp	$t\bar{t}$	top-jets (XC12), p_T>400	XCone-groomed jet mass
2004.00602 5.02 TeV pp/PbPb	jets	q/g-jets (AK4), p_T>120	Jet charge
2101.0472 5.02 TeV pp/PbPb	dijets	q/g-jets (AK4), p_T>50	Jet shapes
2109.0334 13 TeV pp	dijets Z+jets	q/g-jets (AK4), p_T>30 q-jets (AK4), p_T>30	Generalised angularities
2210.08547 5.02 TeV pp/PbPb	jets	q/g-jets, b-jets (AK4), p_T>120	Jet shapes
2211.01456 13 TeV pp	$t\bar{t}$	top-jets (XC12), p_T>400	XCone-groomed jet mass
2312.16343 13 TeV pp	dijets	q/g-jets (AK4, AK8), p_T>700	Lund plane
2312.17103 13 TeV pp	Jets	q/g-jets (AK4), p_T>550	2D angular correlations
2402.13864 13 TeV pp	dijets	q/g-jets (AK4), 97<p_T<1784	Energy correlators
2405.02737 5.02 TeV pp/PbPb	γ+jet	q/g-jets (AK2), p_T>40	Groomed jet radius, girth

See LHC substructure measurements TWiki

Measurement of the primary Lund jet plane density in proton-proton collisions at $\sqrt{s}$ = 13 TeV

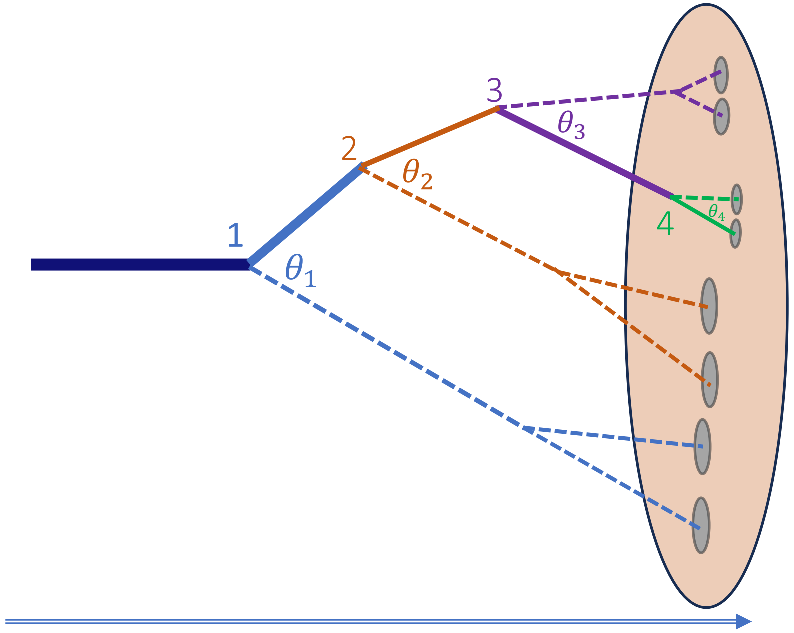

Cambridge-Aachen declustering ($\theta_{i+1} < \theta_i$)

JHEP 05 (2024) 116

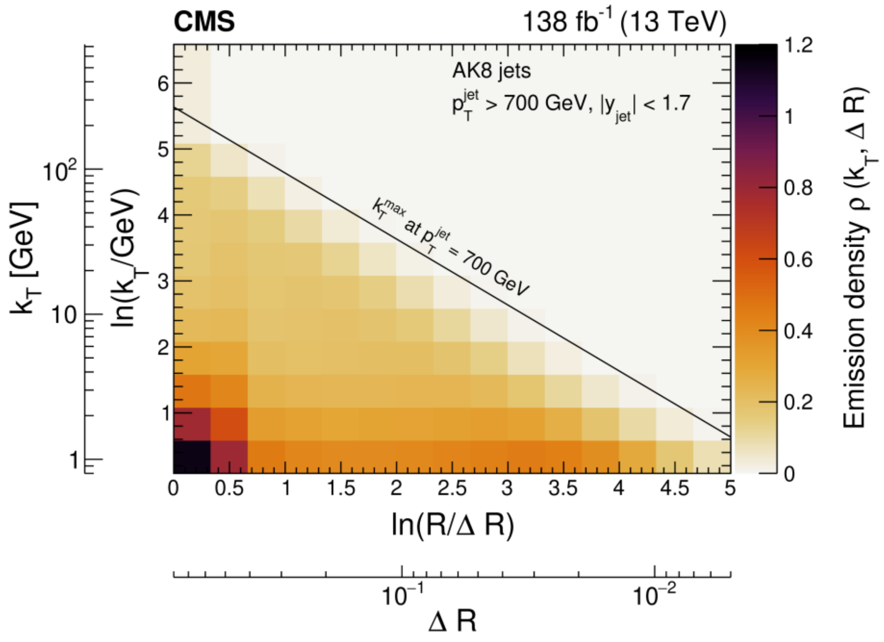

Building the primary Lund jet plane

F. Dreyer, G. Salam, G. Soyez, JHEP 12 (2018) 064

- Angle-ordered reclustering of particles in a jet using Cambridge-Aachen (C/A) algorithm
- Start with the full jet, work backwards through the C/A clustering tree

  → decluster object at step i, store kinematic coordinates characterizing the declustering $\left\{k_T^{(i)}, \Delta R^{(i)}, \ldots\right\}$

$$\Delta R = \sqrt{\left(y_{softer} - y_{harder}\right)^2 + \left(\phi_{softer} - \phi_{harder}\right)^2}\ , \qquad k_T = p_{T,softer} \Delta R$$

  → repeat along the harder of two branches until only 1 particle left on hard branch

Building the primary Lund jet plane

F. Dreyer, G. Salam, G. Soyez, JHEP 12 (2018) 064

- Angle-ordered reclustering of particles in a jet using Cambridge-Aachen (C/A) algorithm
- Start with the full jet, work backwards through the C/A clustering tree

  → decluster object at step i, store kinematic coordinates characterizing the declustering $\left\{k_T^{(i)}, \Delta R^{(i)}, \ldots\right\}$

$$\Delta R = \sqrt{(y_{softer} - y_{harder})^2 + (\phi_{softer} - \phi_{harder})^2}\ , \qquad k_T = p_{T,softer}\Delta R$$

  → repeat along the harder of two branches until only 1 particle left on hard branch

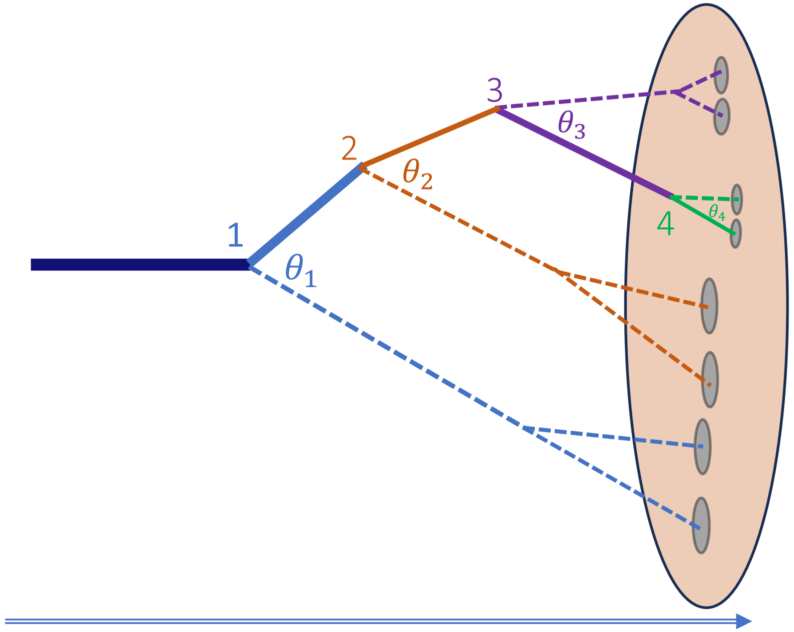

Cambridge-Aachen declustering ($\theta_{i+1} < \theta_i$)

- Ordered list of tuples of kinematic variables fills the primary Lund plane

  from left to right, (from larger to smaller splitting angles)

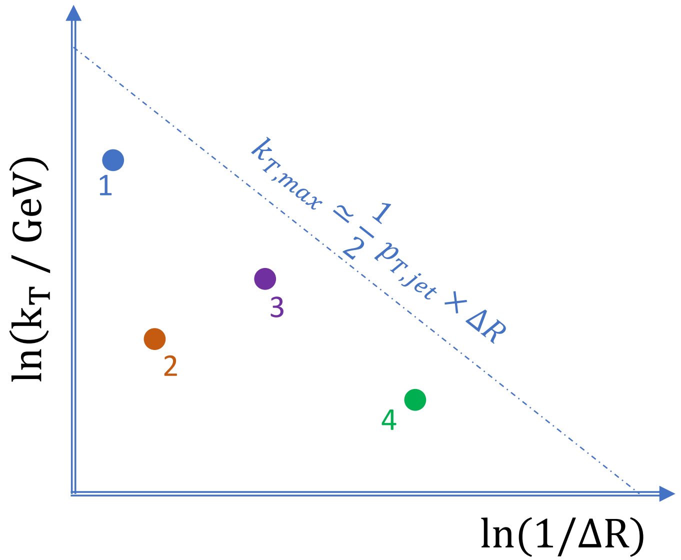

- See Cristian's talk on isolating a gluon-enriched phase space using the secondary LJP!
- Measurements by ATLAS Phys. Rev. Lett. 124, 222002 (2020) and ALICE ALICE-PUBLIC-2021-002

Building the primary Lund jet plane

F. Dreyer, G. Salam, G. Soyez, JHEP 12 (2018) 064

- Angle-ordered reclustering of particles in a jet using Cambridge-Aachen (C/A) algorithm
- Start with the full jet, work backwards through the C/A clustering tree

  → decluster object at step i, store kinematic coordinates characterizing the declustering $\left\{k_T^{(i)}, \Delta R^{(i)}, \ldots\right\}$

  $$\Delta R = \sqrt{(y_{softer} - y_{harder})^2 + (\phi_{softer} - \phi_{harder})^2}\ , \qquad k_T = p_{T,softer}\Delta R$$

  → repeat along the harder of two branches until only 1 particle left on hard branch

- Different QCD mechanisms naturally localized to specific regions of the plane

  → test calculations explicitly for different regimes in slices of k_T and ΔR

  → study specific aspects of mismodeling in MC event generators and parton shower/hadronization models and UE tunes

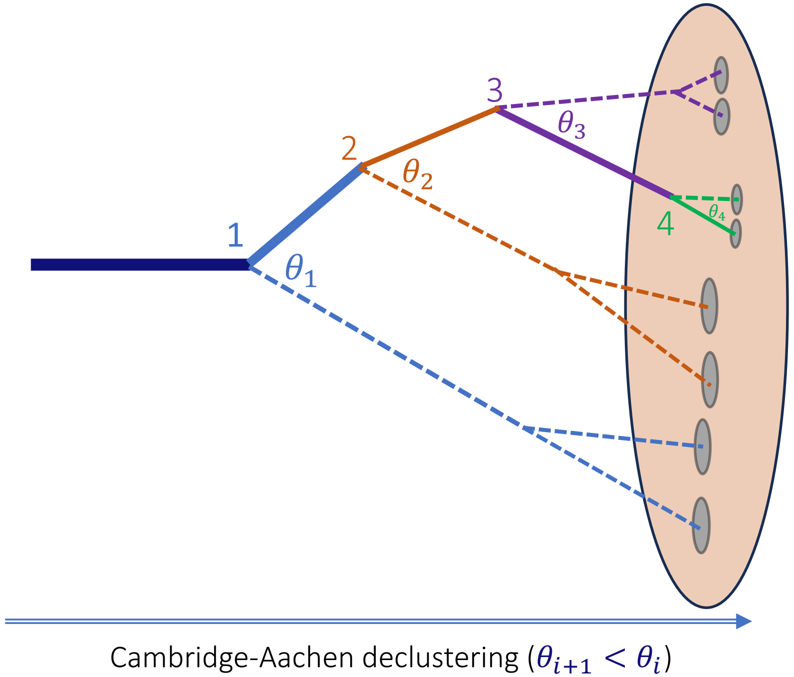

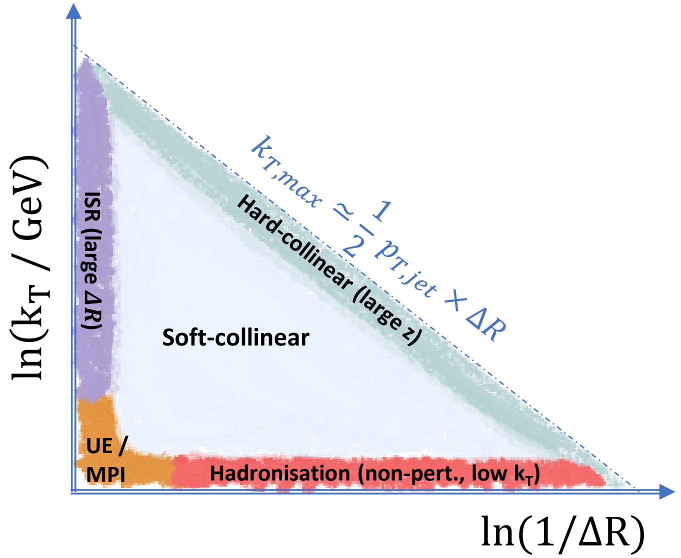

LJP: CMS measurement in Run 2

JHEP 05 (2024) 116

- Inclusive jet selection, with central, high p_T jets:

  → $p_T > 700$ GeV, $|y| < 1.7$

  → anti-k_T jets with $R = 0.4$ and 0.8 (larger PS for hard & wide-angle emissions)

  range of the measurement:

  $\sim 0.4(1) < k_T < \sim 300(700)$ GeV, $0.005 < \Delta R < 0.4(0.8)$

  → pileup (PU) mitigation using charged-hadron subtraction (CHS)

  → negligible background contributions from non-QCD processes,

  → only charged constituents/PF candidates:

  improved angular & momentum resolution

  PU contributions better controlled

- First measurements in large-radius jets; mitigates clustering effects in large swathes of the plane

- HEPData entry available for unfoldings

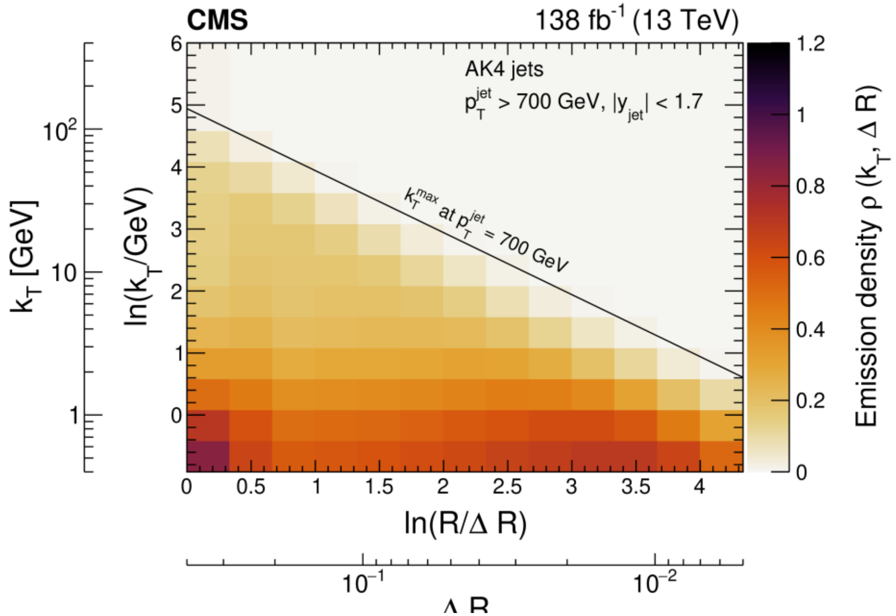

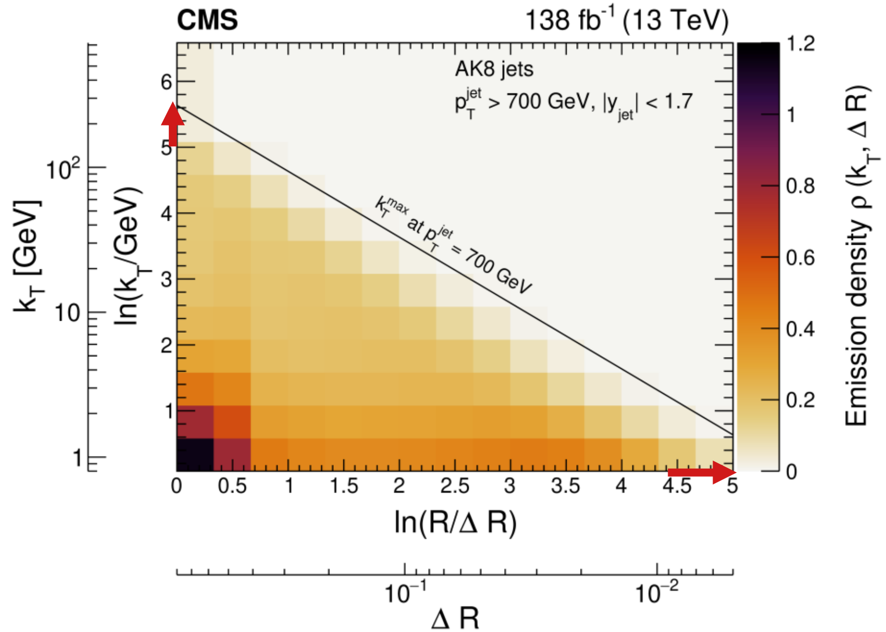

LJP: CMS measurement in Run 2

JHEP 05 (2024) 116

NB: 1-D slices are at the **detector level**, and LJP density after unfolding to the **particle level**

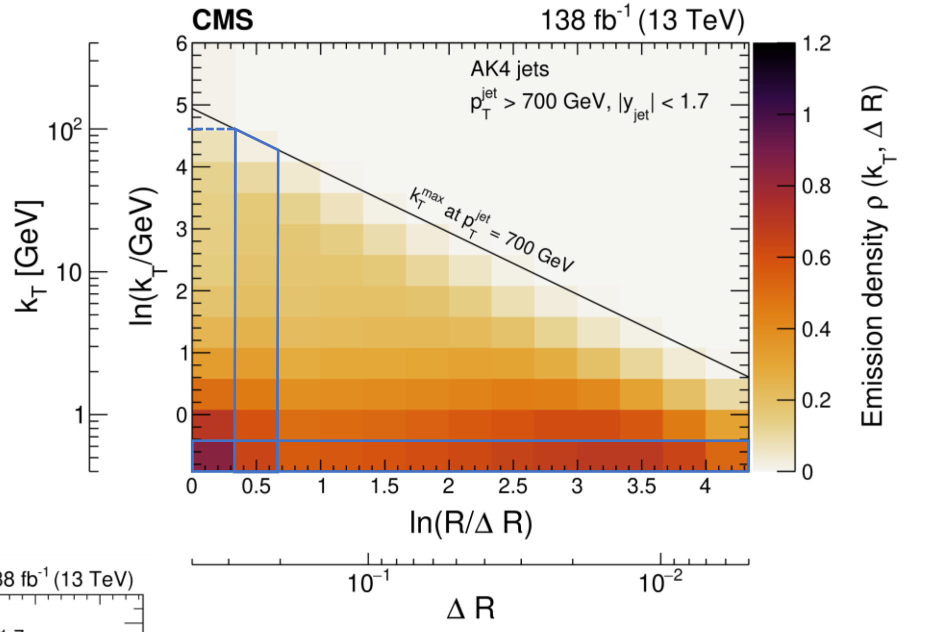

- Measurements are unfolded to particle level
  - → PYTHIA8 CP5 and HERWIG7 CH3 generally envelope data at **detector level** except in low k_T slice
  - → migration matrices and other corrections to detector level derived in nominal MC (PYTHIA8 w. CP5 tune),

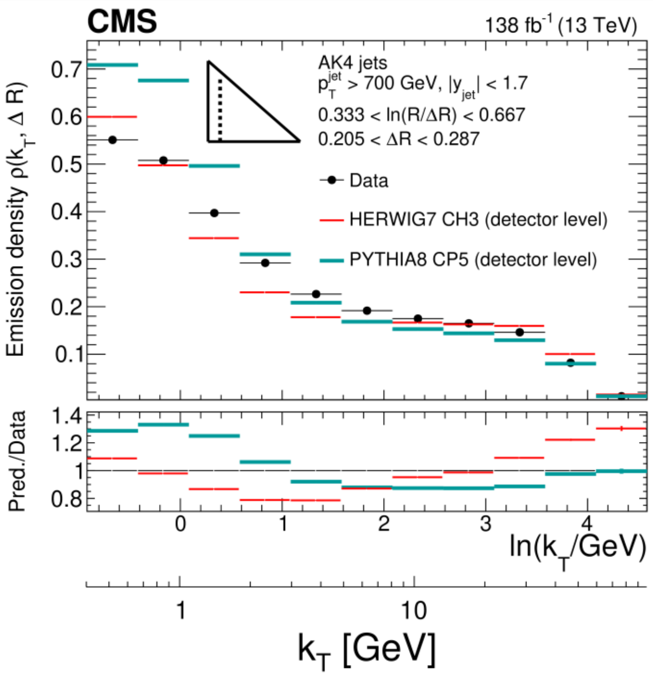

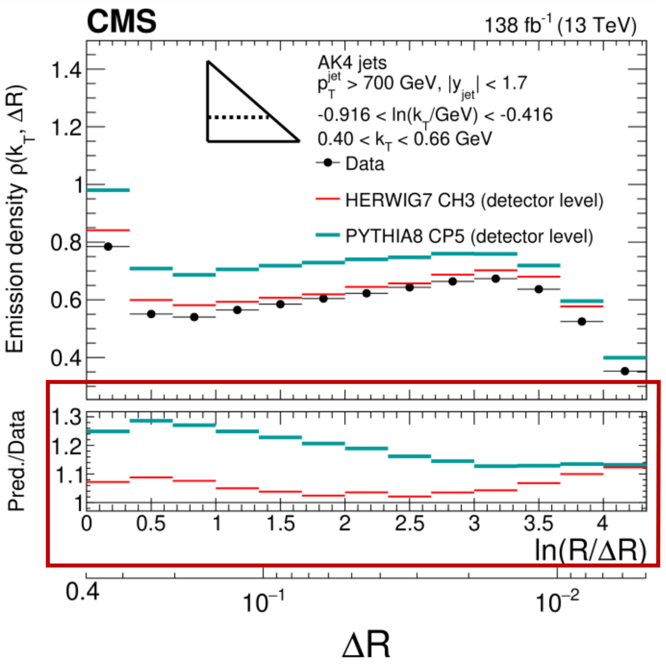

LJP: Handles on PS models and UE tunes

JHEP 05 (2024) 116

Large angles

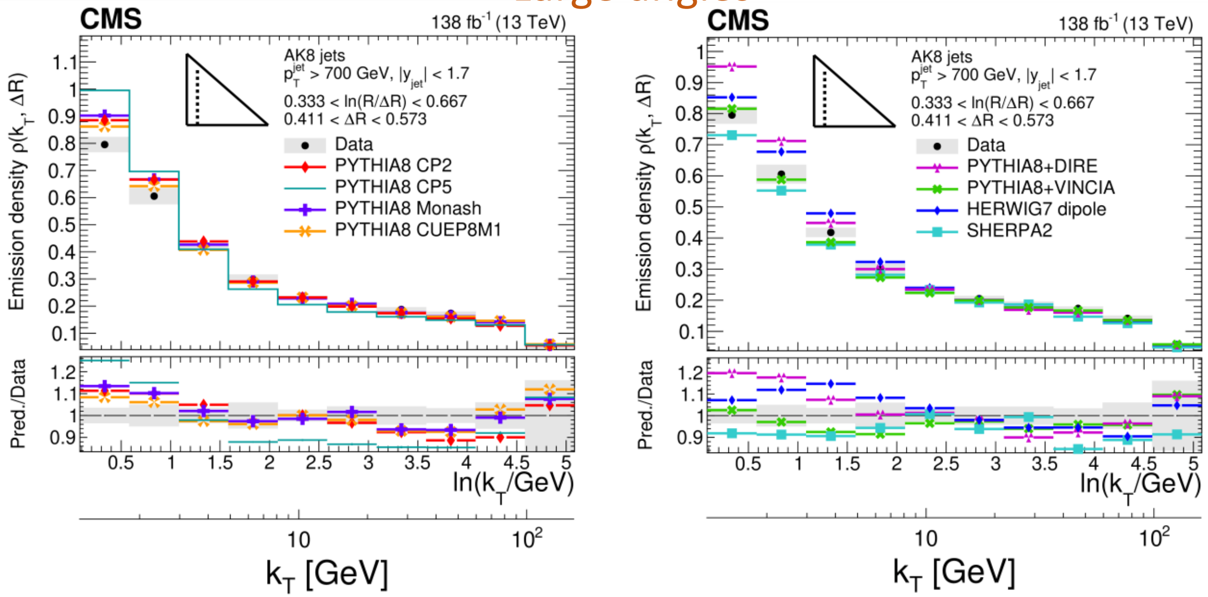

Low k_T (hadronization region)

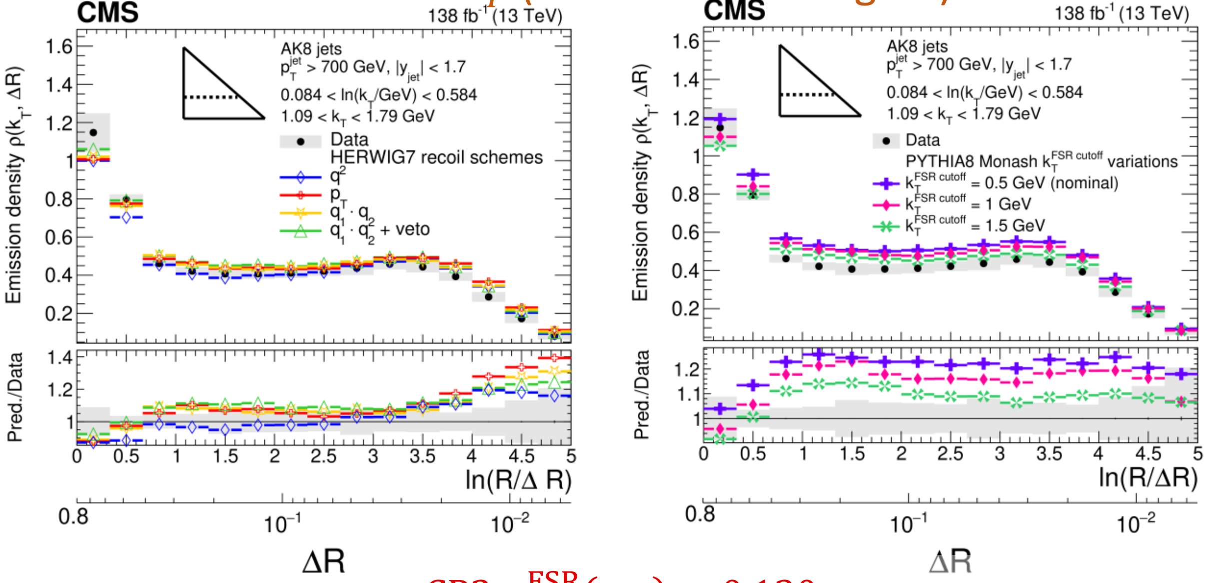

CP2 $\alpha_S^{FSR}(m_Z) = 0.130$
CP5 $\alpha_S^{FSR}(m_Z) = 0.118$
Monash $\alpha_S^{FSR}(m_Z) = 0.1365$
CUEP8M1 $\alpha_S^{FSR}(m_Z) = 0.1365$

- Extensive set of tune/parton shower model comparisons
  - → PYTHIA8 tunes: CP5, CP2, Monash, CUEP8M1
  - → dipole shower models: VINCIA, DIRE, HERWIG7 dipole, SHERPA
  - → angle-ordered Herwig7.2 recoil schemes: q^2, p_T, $q_1 \cdot q_2$, $q_1 \cdot q_2$+veto
  - → variations of k_T^{FSR} cutoff in Monash tune: 0.5, 1, 1.5 GeV
- Differences, all MC, $\sim 10\text{–}20\%$ vs. bulk of the distribution in unfolded data

- Higher values of $\alpha_S^{FSR}(m_Z)$ and k_T^{FSR} describe substructure better
- Angle-ordered showers in HERWIG7 more compatible with data vs. dipole shower across bulk of LJP; (q^2) $q_1 \cdot q_2$+ veto scheme better in (non-)perturbative region,

LJP: Constraining emission patterns in a jet

JHEP 05 (2024) 116

- Comparison to parton level pQCD predictions in measurement phase space

  → **NLL** accuracy, matched to **NLO**, with **NP** corrections

  → ρ scaled by avg. charged fraction (0.62)

  → bin-by-bin correction to hadron level with MC

  → theory uncertainties: from pQCD calculation and NP corrections

  → resummation of non-global logs ↔ increased density at large ΔR

  effect of non-perturbative corrections ↔ at low $k_{\mathrm{T}}(<5\ \mathrm{GeV})$

Analytical calculations of substructure consistent with unfolded data;

precision measurement ↔ our understanding of radiation in jets!

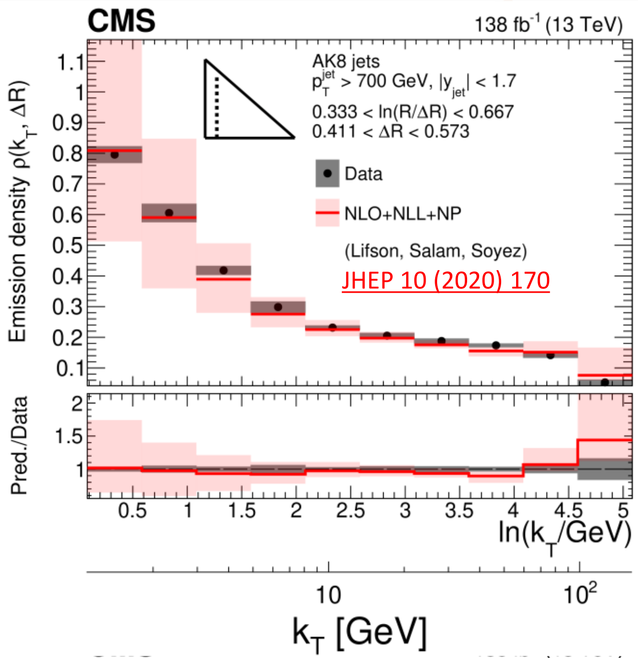

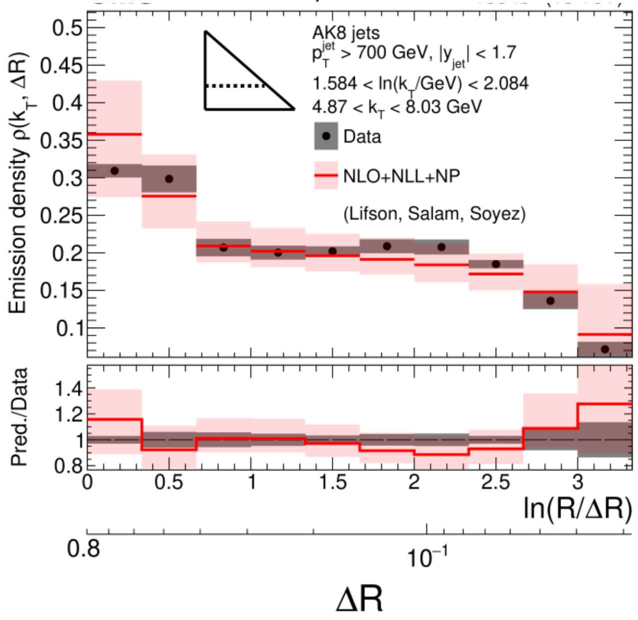

Measurement of energy correlators inside jets and determination $\alpha_S(m_Z)$

arXiv:2402.13864

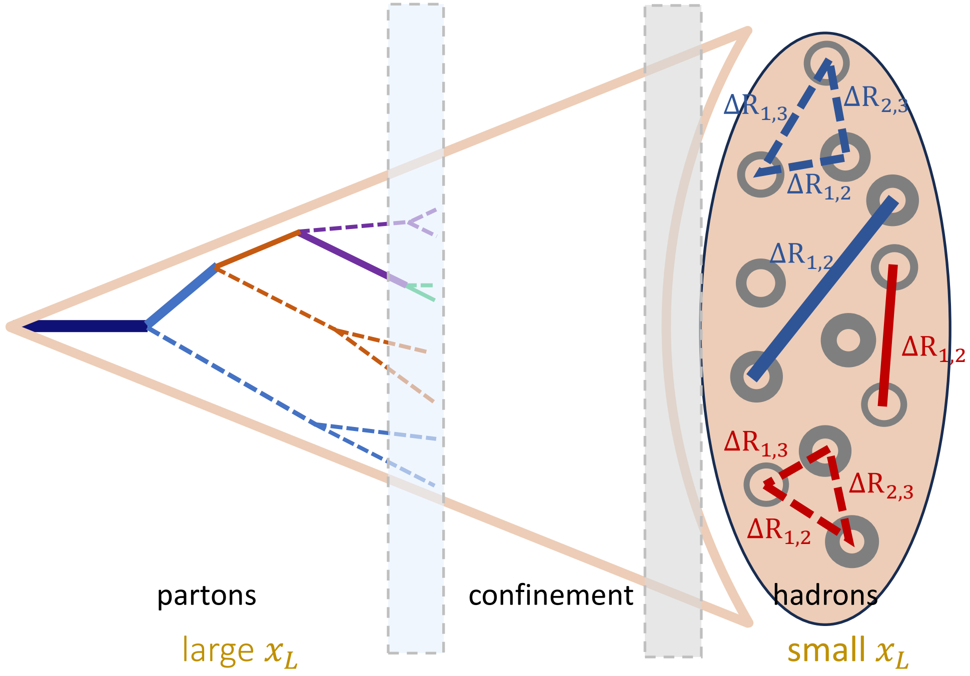

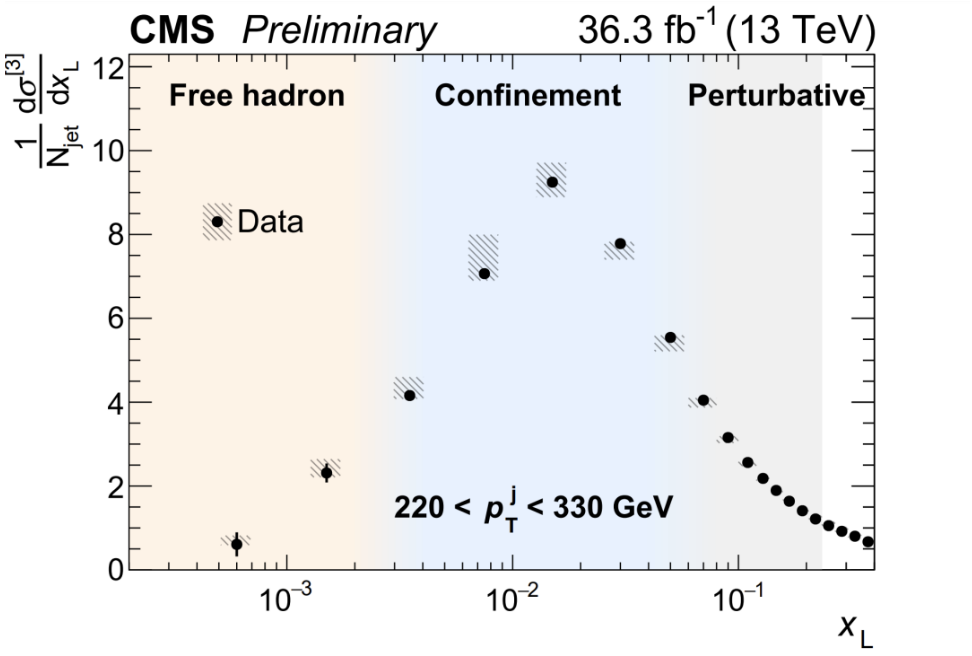

Energy correlators in jets

- Unravel dynamics of jet formation, probe scaling behaviour of QCD

  → jet substructure ↔ study of correlation functions of energy flow operators in the collinear limit (plane of detector cells effectively at infinity)

$$\epsilon(\vec{n}) = \int_0^\infty dt \lim_{r\to\infty} r^2\, n^i T_{0i}\,(t, r\vec{n})$$

  → $\langle\psi|\epsilon(\hat{n}_1)\,\ldots\,\epsilon(\hat{n}_N)|\psi\rangle$, perturbatively calculable at higher orders

  → n-point energy correlators, projected onto axis of (**largest) angular distance** x_L:

$$\text{EnC} = \frac{d\sigma^{[n]}}{dx_L} = \sum_n \sum_{1\le i_1\ldots i_N \le n} \int d\sigma \underbrace{\frac{\prod_{a=1}^N E_{i_a}}{E^N}}_{\text{energy weight}} \delta(x_L - \max\{\Delta R_{i_1,i_2} \ldots \Delta R_{i_{N-1},i_N}\})$$

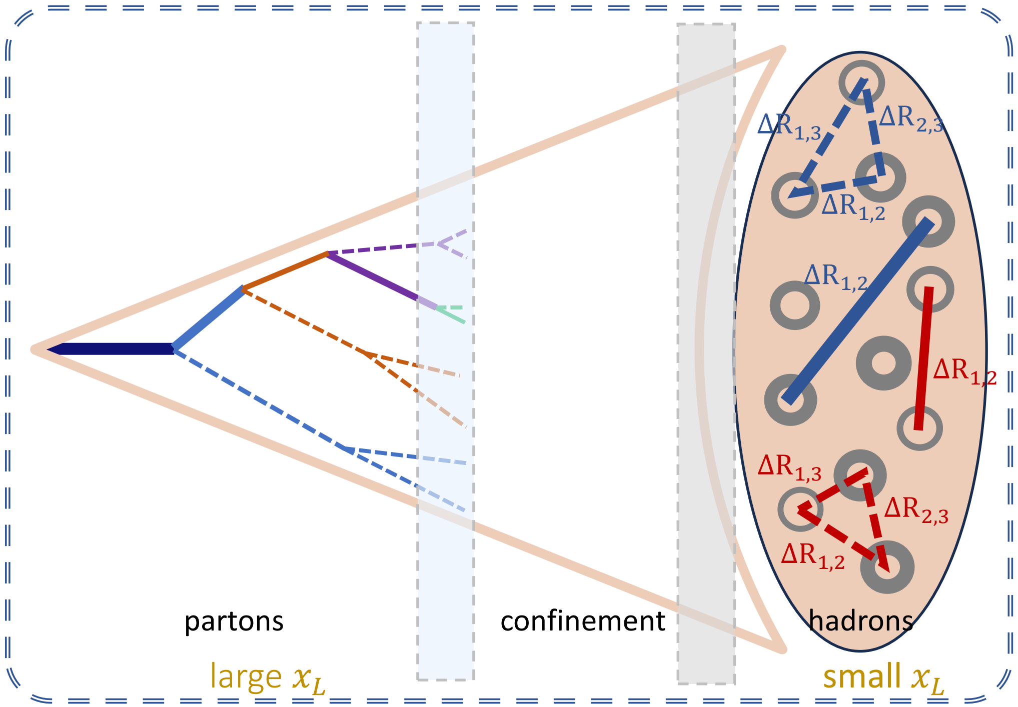

Hofman, Maldacena; JHEP 05 (2008) 012

Dixon, Moult, Zhu; Phys. Rev. D 100, 014009

Chen, Moult, Zhang, Zhu; Phys. Rev. D 102, 054012

Chen, Luo, Moult, Yang, Zhang, Zhu; JHEP 08 (2020) 028

Lee, Meçaj, Moult; arXiv:2205.03414

Energy correlators in jets

- Unravel dynamics of jet formation, probe scaling behaviour of QCD

  → jet substructure ↔ study of correlation functions of energy flow operators in the collinear limit (plane of detector cells effectively at infinity)

$$\epsilon(\vec{n}) = \int_0^\infty dt \lim_{r\to\infty} r^2\, n^i T_{0i}\,(t, r\vec{n})$$

  → $\langle\psi|\epsilon(\hat{n}_1)\,\ldots\,\epsilon(\hat{n}_N)|\psi\rangle$, perturbatively calculable at higher orders

  → n-point energy correlators, projected onto axis of (**largest) angular distance** x_L:

energy weight

$$EnC = \frac{d\sigma^{[n]}}{dx_L} = \sum_n \sum_{1\le i_1\ldots i_N \le n} \int d\sigma \frac{\prod_{a=1}^N E_{i_a}}{E^N}\, \delta\left(x_L - \max\{\Delta R_{i_1,i_2} \ldots \Delta R_{i_{N-1},i_N}\}\right)$$

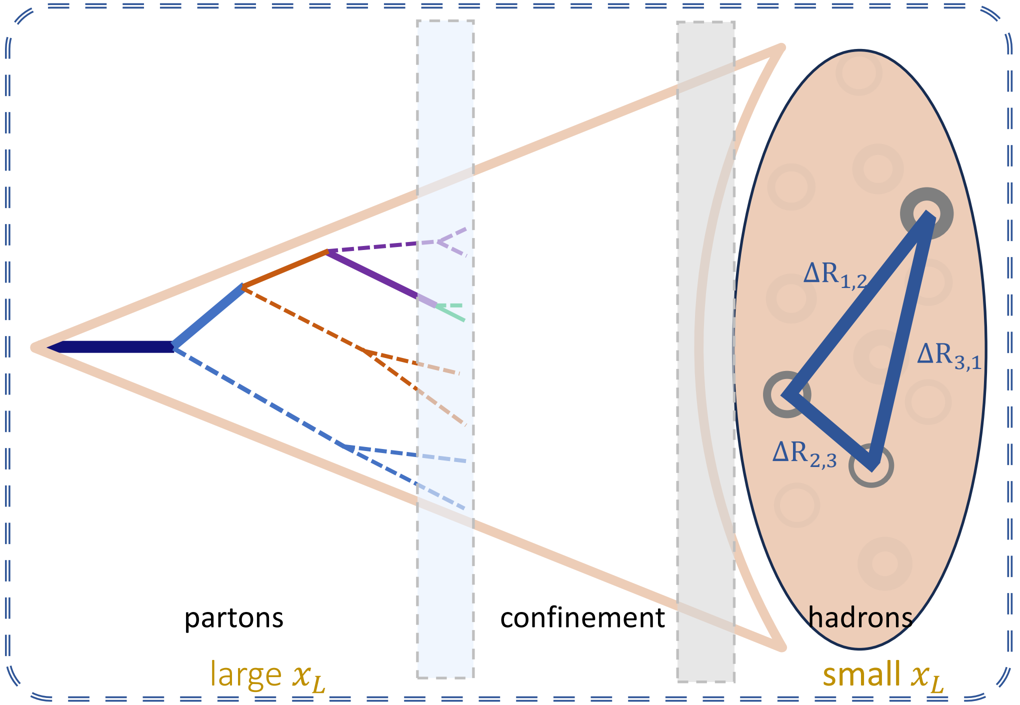

- Multi-entry distributions for correlations between pairs/triplets of emissions

- Amenable to a novel extraction of the strong coupling

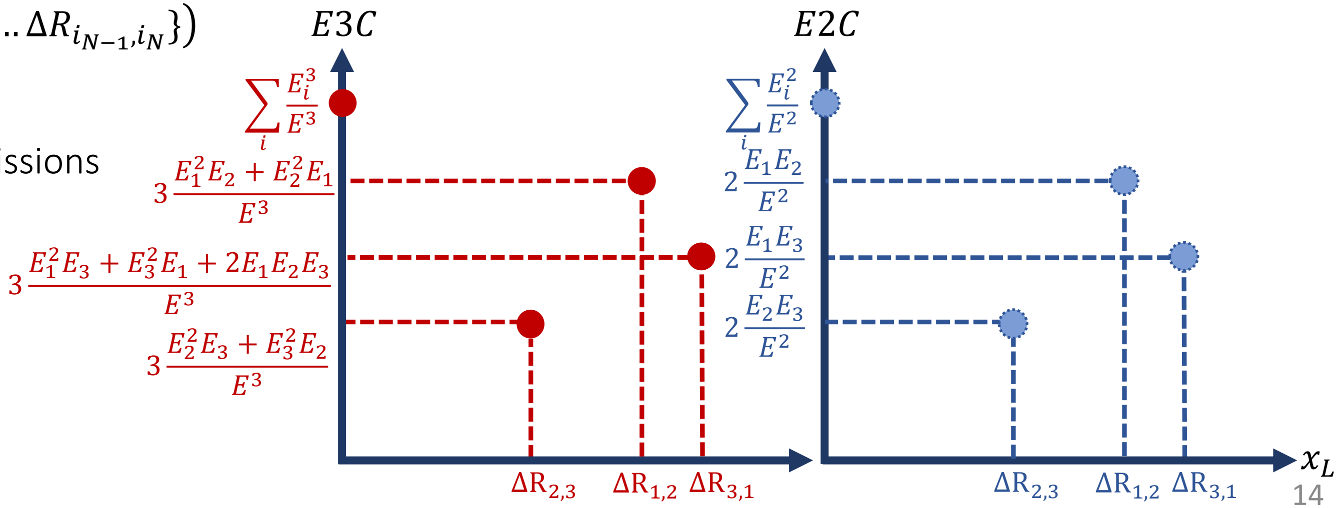

Energy correlators in jets

- Substructure measurements of α_S complicated by degeneracies between α_S and q/g fractions in jets (emission probabilities $\propto \alpha_S\, C_i$)

- **Linear** dependence on strong coupling at leading log:

$$\mathrm{E2C, E3C} \sim \mathrm{c}_0 + \mathrm{c}_1 \alpha_S(Q)\ln(x_L) + O\left(\alpha_S^2\right) + (\ldots),$$

  → different c_i's for E2C and E3C, dependent on color factors C_i and q/g fractions

$$\frac{\mathrm{E3C}}{\mathrm{E2C}} = \frac{d\sigma^{[3,2]}}{dx_L} \propto \alpha_S(Q)\ln(x_L) + O\left(\alpha_S^2\right),$$

  → ratio mitigates dependence on q/g fraction, robust to detector effects, cancellation of PDF uncertainties, highlights dependence on $\alpha_S(Q)$

- Scale uncertainties still large at NLL due to perturbative corrections, with effect of corrections greatly reduced at NNLL accuracy

$Q \sim p_{T,\mathrm{jet}} \cdot x_L$

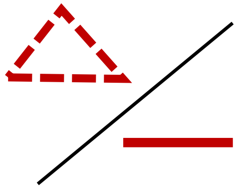

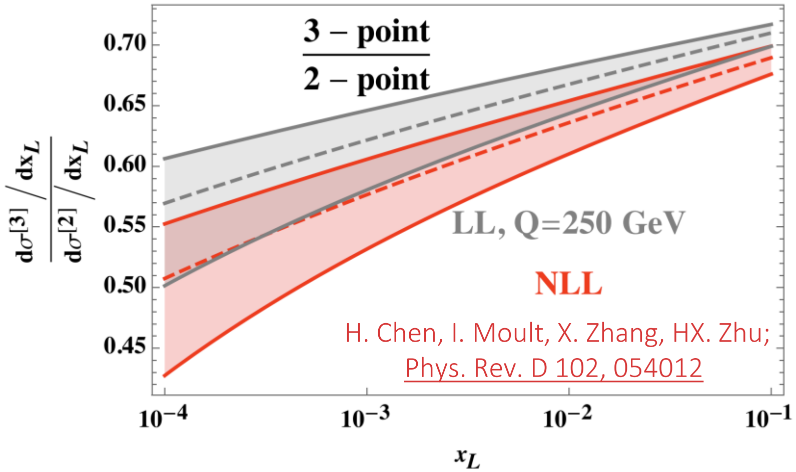

H. Chen, I. Moult, X. Zhang, HX. Zhu; Phys. Rev. D 102, 054012

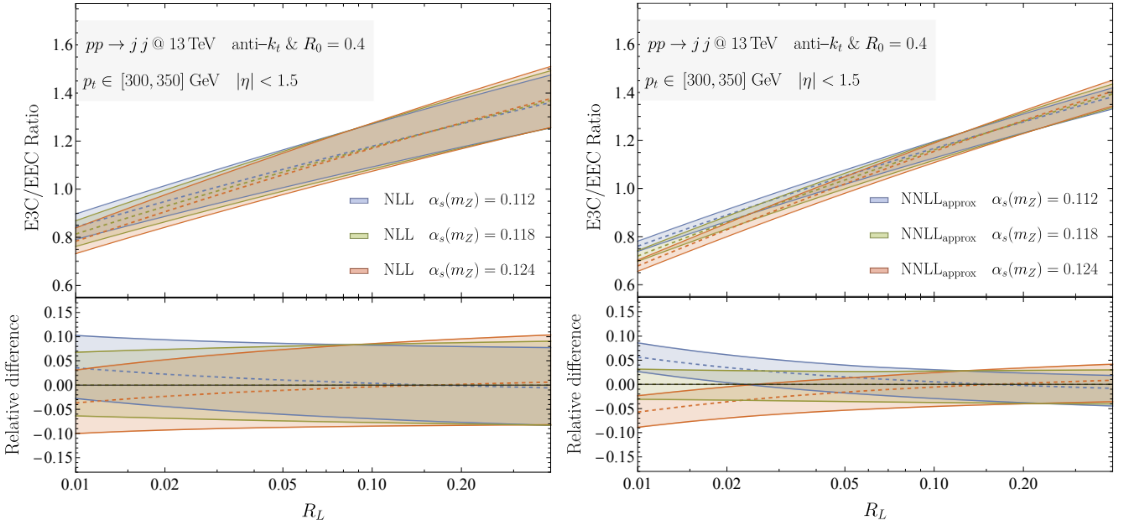

W. Chen, J. Gao, Y. Li, Z. Xu, X. Zhang, HX. Zhu; JHEP 05 (2024) 043

ENC: CMS measurement in Run 2

arXiv:2402.13864

- Inclusive jet selection requiring at least 2 jets:

  → $97 < p_T < 1784$ GeV (8 regions), $|\eta| < 2.1$, $|\Delta\phi\,(j_1, j_2)| > 2$,
  → anti-k_T jets with $R = 0.4$ ($Q \sim p_{T,\text{jet}}\, x_L$: $5 - 80$ GeV)
  → negligible background contributions from non-QCD physics processes
  → charged-hadron subtraction (CHS)
  → **neutral and charged particles** with $p_T > 1$ GeV
  → measurement in 2016 data (36.3 fb^{-1}), enough events for precision, low PU

- First measurement of 3-point correlator, and extraction of strong coupling using E3C/E2C ratio

- Slope measurements of ratio vs. $\ln(x_L)$ sensitive to α_S

  → study in slices of p_T to probe running of the coupling with energy scale

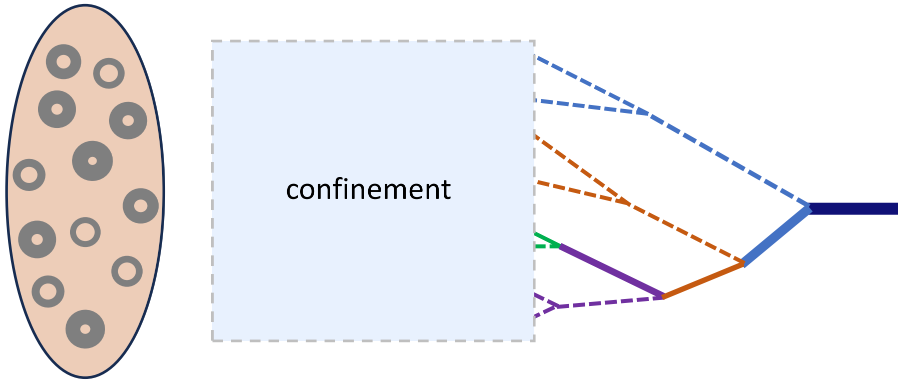

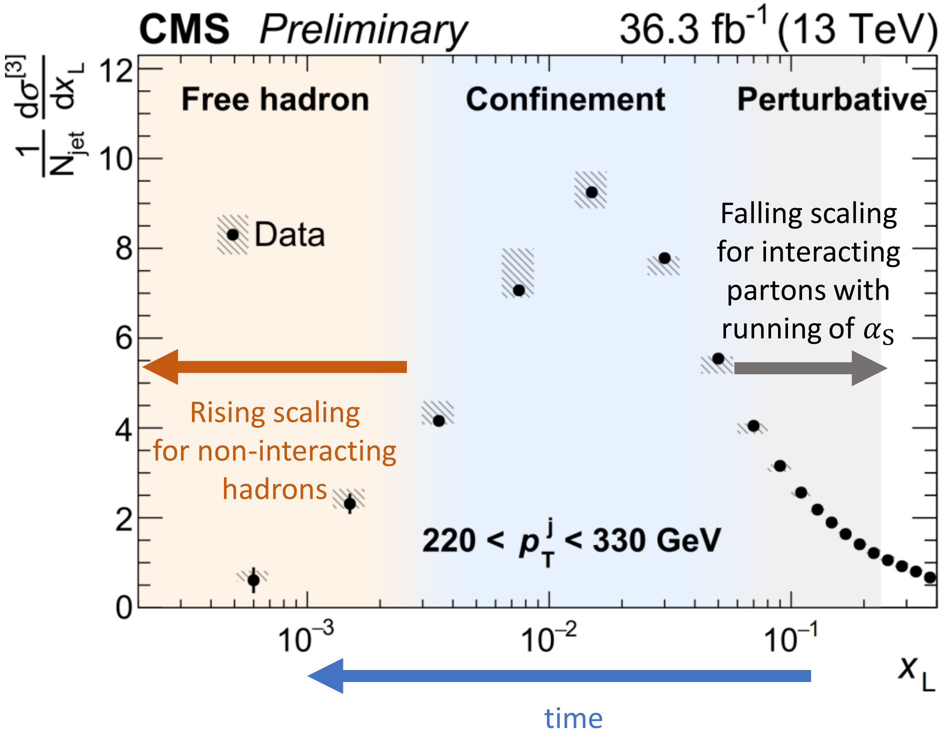

E3C/E2C: Unfolded measurements

arXiv:2402.13864

$Q \propto x_L \cdot p_{T,\mathrm{jet}}$: Boundaries between regions shift to smaller x_L at high p_T

- Uncertainties and disagreements with data **reduced** in ratio E3C/E2C vs. x_L
  - → ∼10% data/MC disagreement reduced to ∼3%
  - → experimental systematics ∼8% reduced to ∼3%
- **Leading contributions** to uncertainties:
  - → shower and model uncertainties
  - → neutral hadron and photon energy scale
- Slope of distributions in perturbative region reduces at larger values of p_T

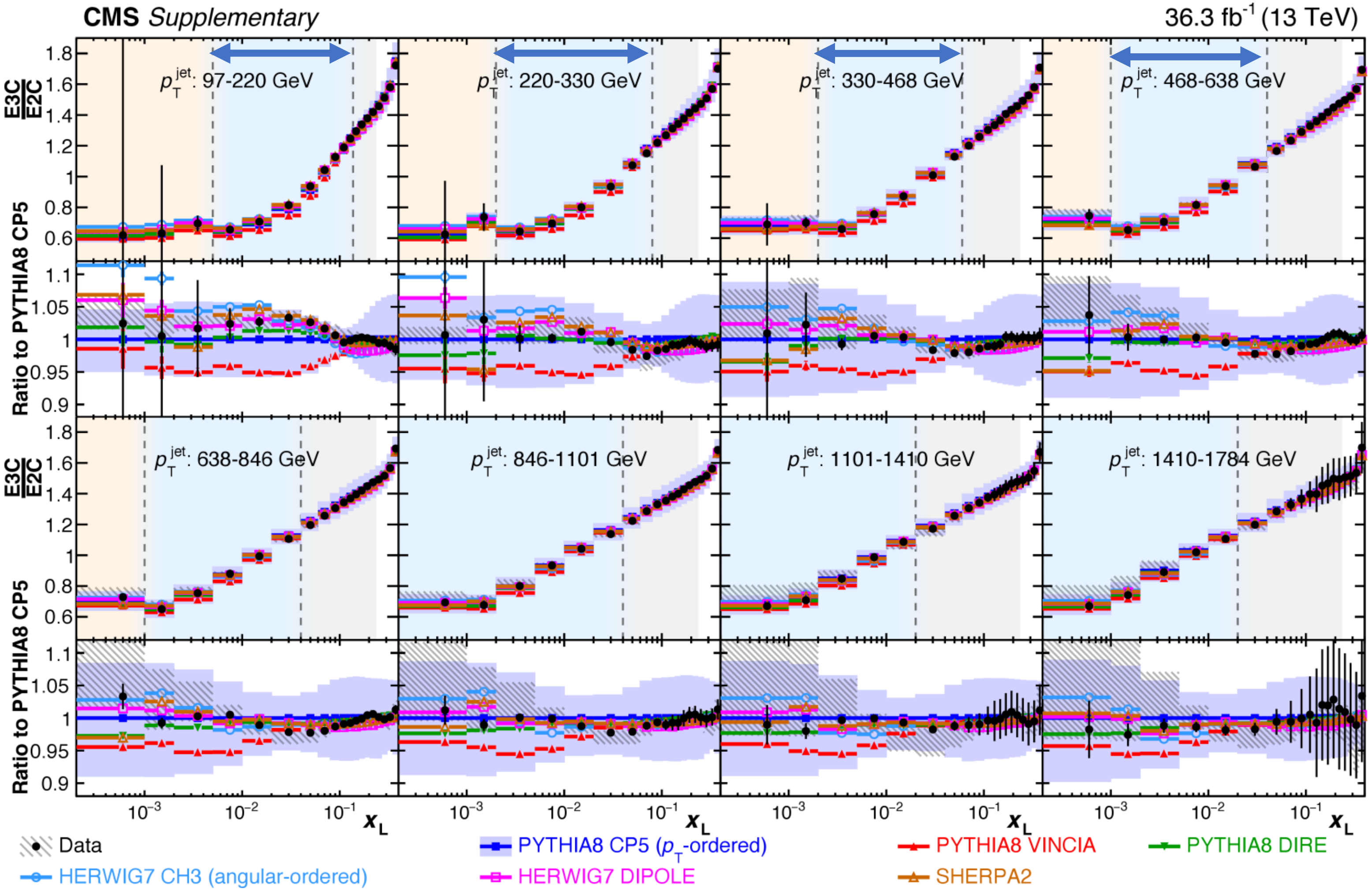

$x_L \simeq \frac{0.8}{p_{T,\mathrm{jet}}}$ ⟷ $x_L \simeq \frac{20}{p_{T,\mathrm{jet}}}$

E3C/E2C: Observation of asymptotic freedom

arXiv:2402.13864

- Slopes of ratios in perturbative region reduces at higher p_T
- Fit $\Delta(E3C/E2C)/\Delta \ln x_L$ in a p_T region, and plot as a function of p_T (x-errors widths of p_T regions)
- Direct observation of asymptotic freedom at large energy scales!
- Comparisons to median values (in x_L) of three different theoretical predictions in perturbative region with variations of $\alpha_S(m_Z)$

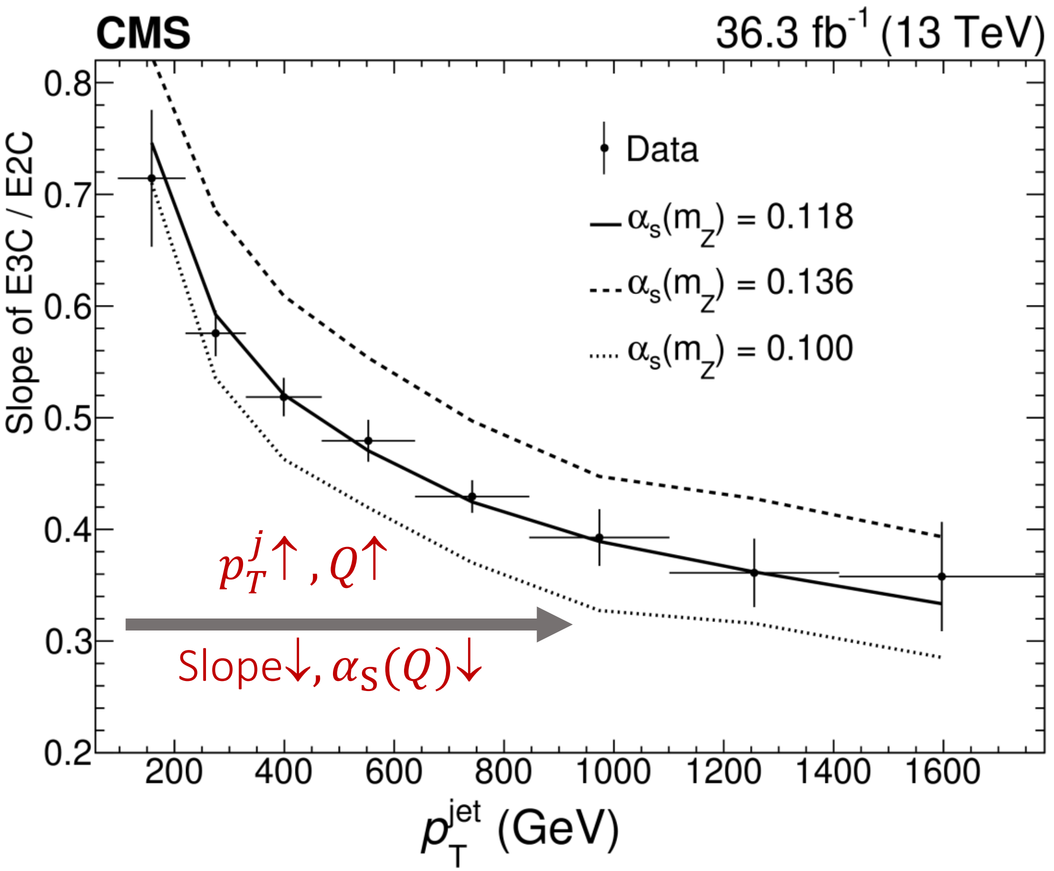

E3C/E2C: Precision extraction of α_S

arXiv:2402.13864

- Direct extraction of coupling from E3C/E2C vs. x_L (pert. regime, $x_L < 0.234$)
- Extraction using comparisons with theoretical predictions at NLO+NNLL$_{\text{approx}}$ for variations of $\alpha_S(m_Z)$
  - → minimize χ^2 between measurement and prediction using total covariance
  - → nuisance parameter for unknown per-p_T bin theory normalization in
  - → nuisance parameters simultaneously varied,
    PS renormalization scale unc. replaced by those for NNLL$_{\text{approx}}$ predictions

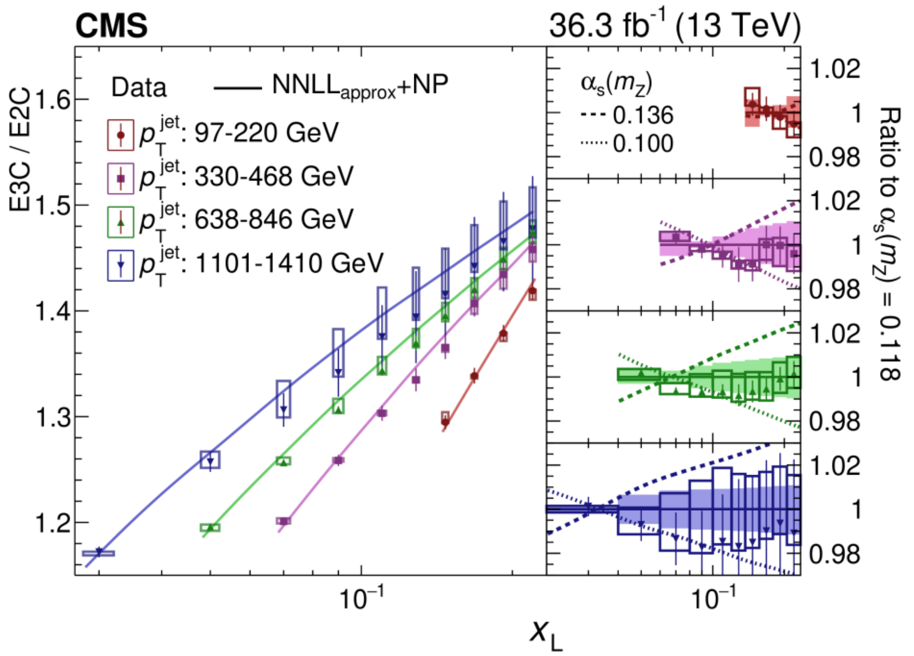

- $$\alpha_S(m_Z) = 0.1229^{+0.0040(\text{stat.})+0.0030(\text{th.})+0.0023(\text{exp.})}_{-0.0012(\text{stat.})-0.0033(\text{th.})-0.0036(\text{exp.})}$$

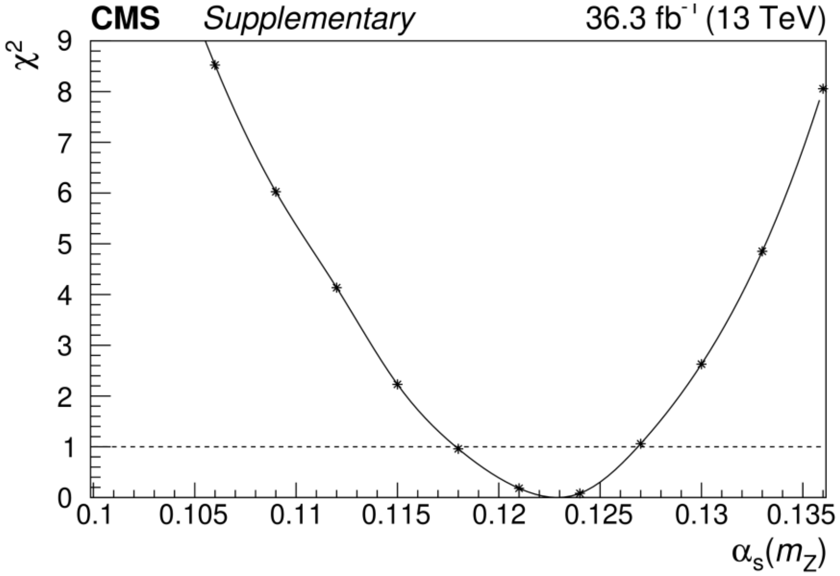

Uncertainties $\sim 4\%$: most precise extraction of α_S leveraging jet substructure

Leading systematics: QCD scale for NLO+NNLL$_{\text{approx}}$ prediction, neutral hadron and photon energy scale

⇒ expect reduction of uncertainties when using charged particle only

Summary

- Precision measurements of per-jet, multi-entry substructure observables:
  $\rightarrow$ sensitivity to fundamental QCD mechanisms over a large range of energy scales
  $\rightarrow$ comparisons to perturbative, higher-order QCD calculations for jet substructure

- Factorisation of effects of QCD phenomena for phase space of emissions in a jet with single observable:
  using iterative declustering, extensive set of **handles to constrain parton showers and analytic predictions**

- Direct sensitivity to time evolution of shower, scaling behaviour of QCD, with objects grounded in field-theory:
  observation of **confinement**, **asymptotic freedom** and **extraction of $\alpha_S(m_Z)$** from multi-particle correlations

- **MC model uncertainties dominant in jet substructure measurements:**
  $\rightarrow$ provide complementary handles for benchmarking and constraining event generators, parton shower and hadronization models in well factorized measurements

BACKUP SLIDES

Primary Lund jet plane density

- Jet-averaged density (ρ) of 1→2 splittings in the Lund plane

  → calculable in perturbative QCD, where at leading order,

  in **soft and collinear limit**, density scales with coupling,

$$\rho(\Delta R, k_T) = \frac{1}{N_{jets}} \frac{d^2 N_{emissions}}{d\ln(k_T\,/\,\text{GeV})\, d\ln(R/\Delta R)} \approx \frac{2}{\pi} C_i \alpha_S(k_T),$$

C_i: Casimir for quarks ($C_F = 4/3$) and gluons ($C_A = 3$)

$$\alpha_S \propto \frac{1}{\ln\left(\frac{k_T}{\Lambda_{QCD}}\right)} \quad \Rightarrow \sim \text{uniform } \rho \text{ at high } k_T,\ \rho\uparrow \text{ at low } k_T \text{ as } \alpha_S \gg 1$$

- Broad features of unfolded LJP density described well **in soft and collinear limit**,

  → simplified assumptions: 1-loop β function with $\alpha_S(m_Z) = 0.118$,

  → effective color factor $C_R = 0.59\, C_F + 0.41\, C_A \approx 2$ (from MC q/g fractions)

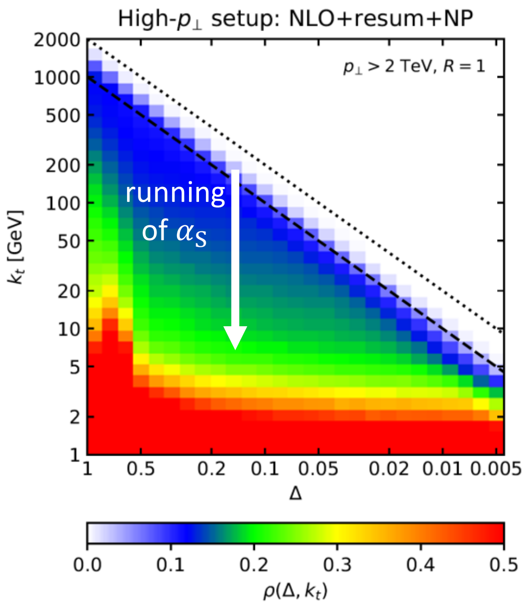

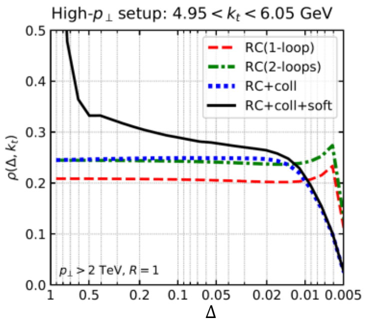

A. Lifson, G. Salam, G. Soyez, JHEP 10 (2020) 170

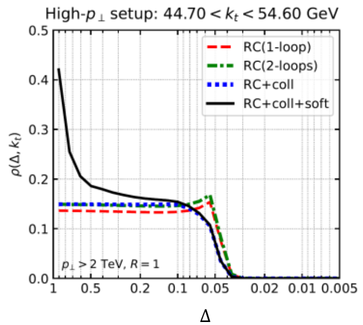

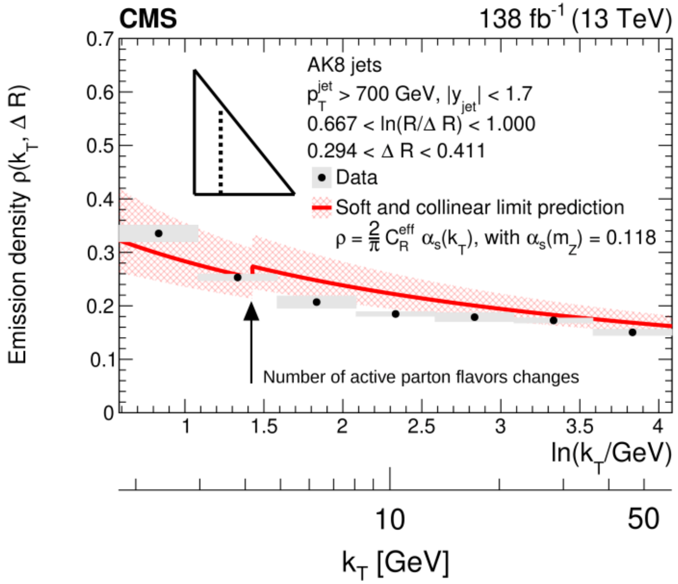

LJP: Unfolding and corrections

[JHEP 05 (2024) 116](https://doi.org/10.1007/JHEP05(2024)116)

- Migration matrix for unfolding with geometric matching of detector- and truth-level jets and matching of emissions

  → match detector- and particle-level splittings in PYTHIA8 CP5; choose closest in $\eta - \phi, \forall\, \Delta R(\triangle,\blacktriangledown) < 0.1$ for multiple matches

  → **background** (bin-by-bin) subtraction of unmatched detector-level emissions estimated in MC (**purity** corrections)

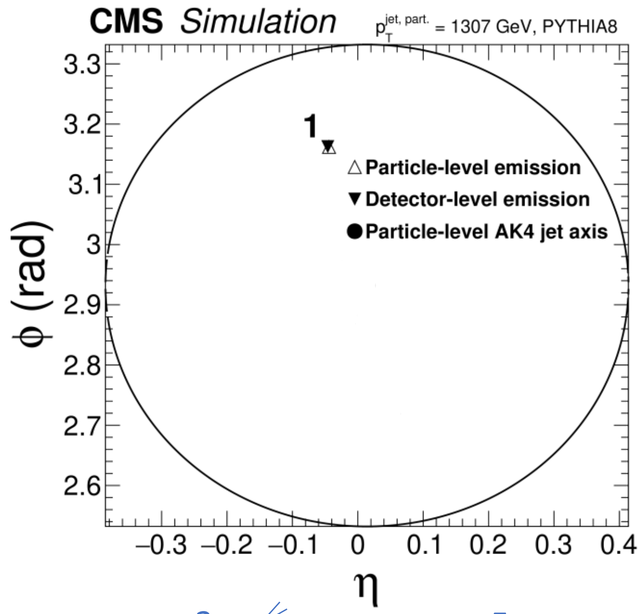

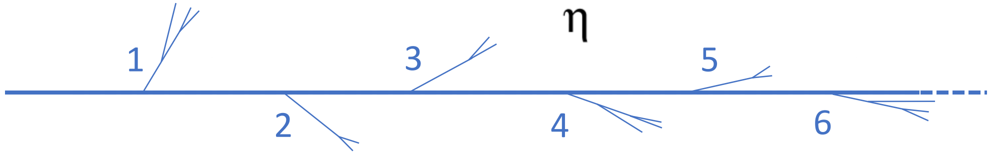

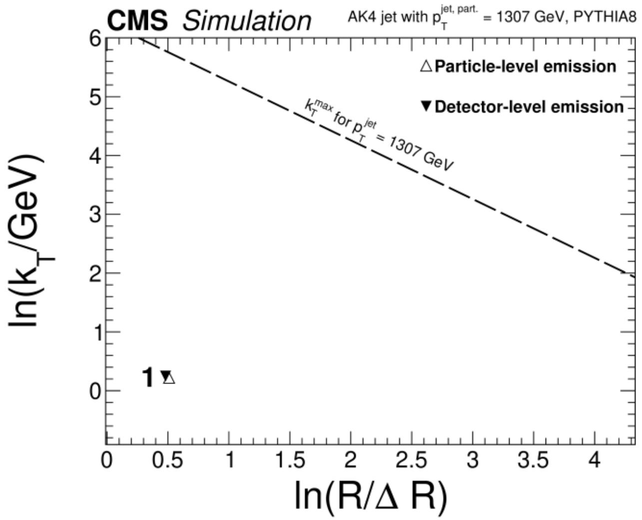

LJP: Unfolding and corrections

JHEP 05 (2024) 116

- Migration matrix for unfolding with geometric matching of detector- and truth-level jets and matching of emissions

  → match detector- and particle-level splittings in PYTHIA8 CP5: choose closest in $\eta - \phi, \forall\ \Delta R(\triangle,\blacktriangledown) < 0.1$ for multiple matches

  → **background** (bin-by-bin) subtraction of unmatched detector-level emissions estimated in MC (purity corrections)

- Primary LJP density unfolded multidimensionally $(p_{\mathrm{T,jet}},\ k_T,\ \Delta R)$

  → Multi-entry distribution, bin-to-bin statistical correlations: $5-10\%$

  → regularized D'Agostini unfolding: minimise χ^2 between input and forward-folded unfolded distribution: 12(8) iterations for R=0.4(0.8)

  → **correction** to N_{jets} for migrations between detector-/generator-level anti-k$_T$ jet p_{T},

  → **efficiency** corrections (bin-by-bin) for unmatched hadron-level emissions in MC

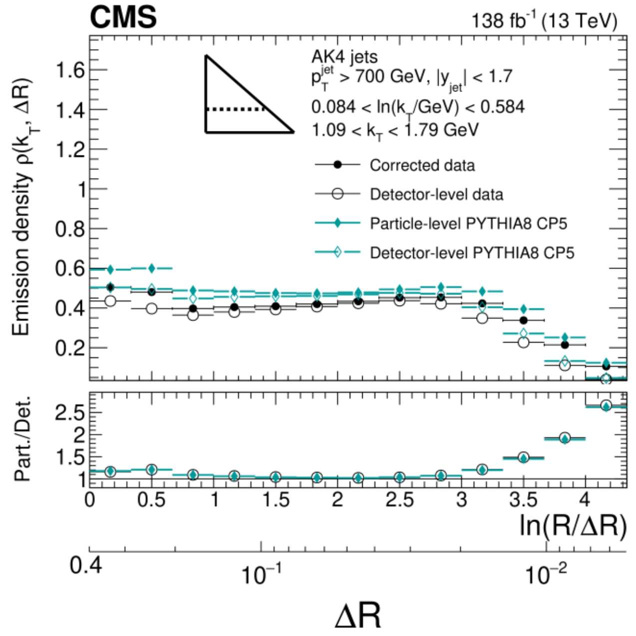

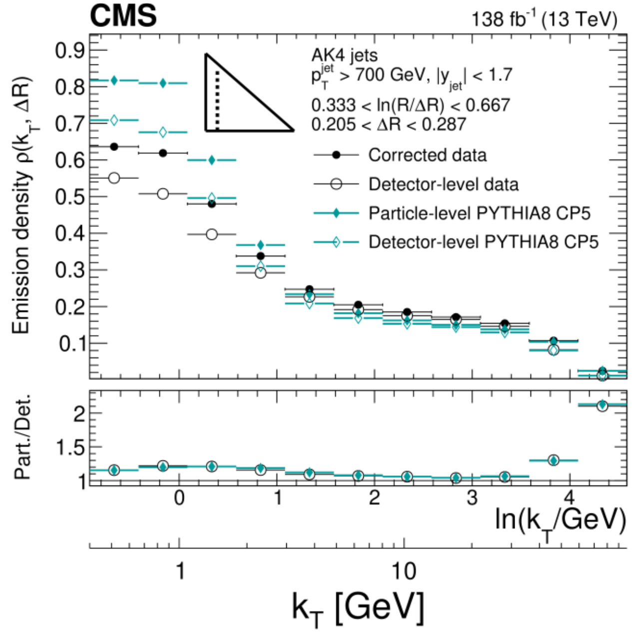

LJP: Unfolding and corrections

JHEP 05 (2024) 116

- Migration matrix for unfolding geometric matching of detector- and truth-level jets, and the matching of emissions
  - → match detector- and particle-level descriptions of splittings in nominal MC (PYTHIA8 CP5): choose closest in $\eta - \phi, \forall\, \Delta R(\triangle, \blacktriangledown) < 0.1$
  - → background (bin-by-bin) subtraction of unmatched detector-level emissions estimated in MC (**purity** corrections)

- Primary LJP measurements unfolded multidimensionally in $\left(p_{\mathrm{T,jet}}, k_{\mathrm{T}}, \Delta R\right)$
  - → bin-to-bin stat. correlations: $5 - 10\%$
  - → regularized D'Agostini unfolding: minimise χ^2 between input and forward-folde distribution: 12(8) iterations for R=0.4(0.8)
  - → correction to N_{jets} for migrations between det.-/gen.-level anti-k_{T} jet p_{T}
  - → efficiency corrections (bin-by-bin) for unmatched hadron-level emissions in MC

Detector level | Particle level

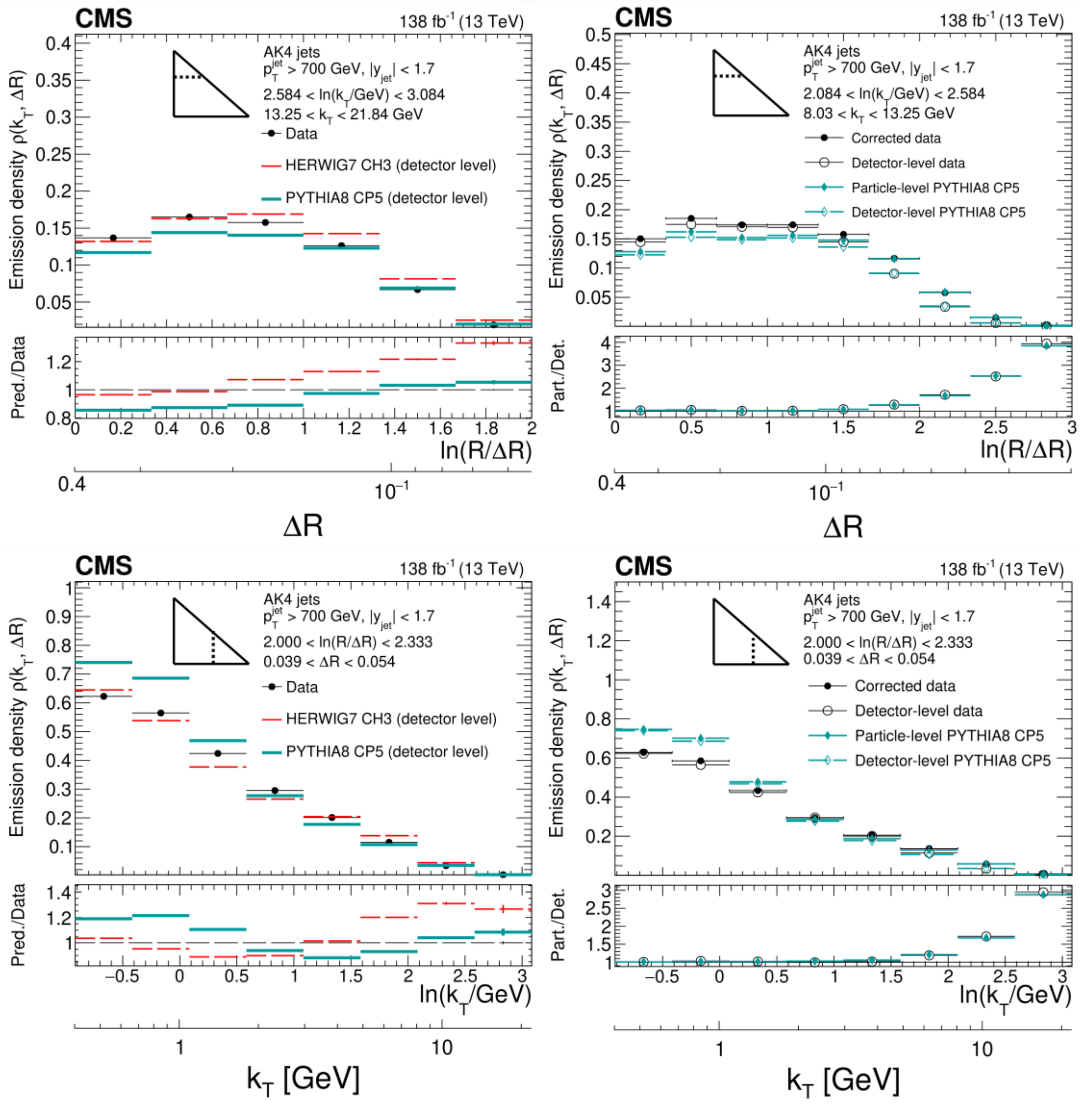

LJP: Unfolding uncertainties

JHEP 05 (2024) 116

- Leading contributions
  - → parton shower + hadronization model uncertainty (dominant in bulk):
    decorrelated MC prior and response matrix stat. contributions in regularized unf.
    swap in HERWIG7 CH3 predictions for the prior/matrix from PYTHIA8 CP5;
    2–7% contribution in bulk, ~20% at kinematic edge of LJP
  - → tracking efficiency uncertainty (dominant at high k_T):
    1-2% contribution in bulk, 15–25% at kinematic edge of LJP/in pert. region;
    includes contributions from losing subjets to cluster merging at $\Delta R \sim 0.05$
    and (at low $k_T, \Delta\mathrm{R}$) $p_T > 1$ GeV requirement for PF cands.
- Sub-percent contributions
  - → parton shower scale
  - → finite statistics of the response matrix
  - → (global) jet energy scale and resolution
  - → pileup modeling

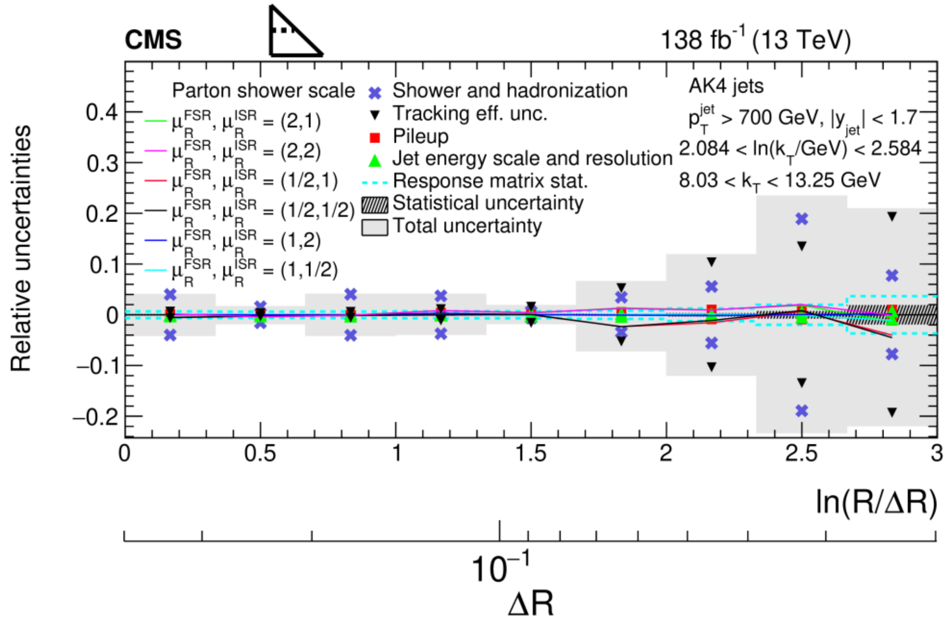

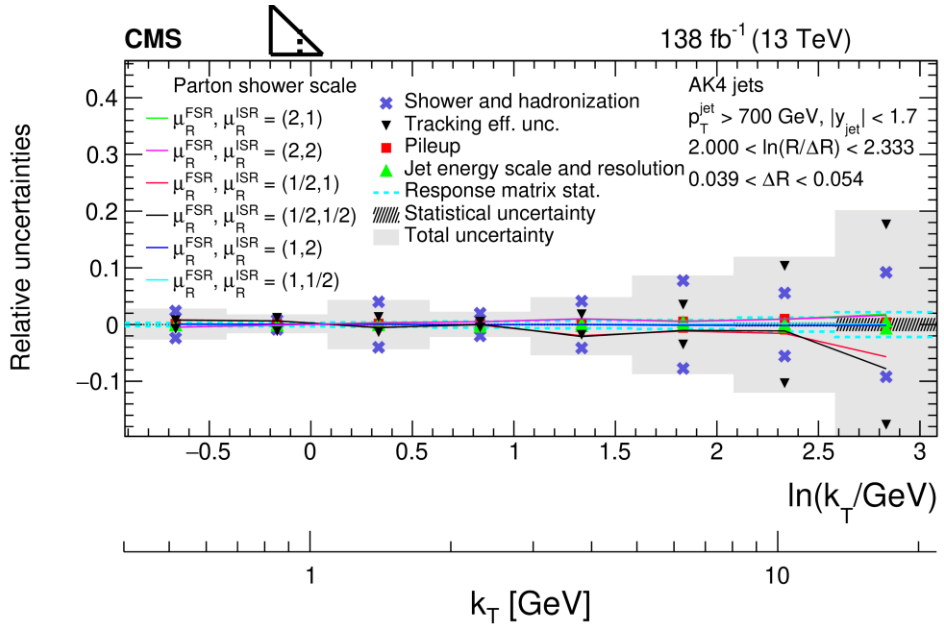

LJP: Unfolding uncertainties

JHEP 05 (2024) 116

- Leading contributions
  - → parton shower + hadronization model uncertainty (dominant in bulk):
    - decorrelated MC prior and response matrix stat. contributions in regularized unf.
    - swap in HERWIG7 CH3 predictions for the prior/matrix from PYTHIA8 CP5;
    - 2–7% contribution in bulk, ~20% at kinematic edge of LJP
  - → tracking efficiency uncertainty (dominant at high k_T):
    - 1-2% contribution in bulk, 15–25% at kinematic edge of LJP/in pert. region;
    - includes contributions from losing subjets to cluster merging at $\Delta R \sim 0.05$
    - and (at low $k_T, \Delta \mathrm{R}$) $p_T > 1$ GeV requirement for PF cands
- Sub-percent contributions
  - → parton shower scale
  - → finite statistics of the response matrix
  - → (global) jet energy scale and resolution
  - → pileup modeling

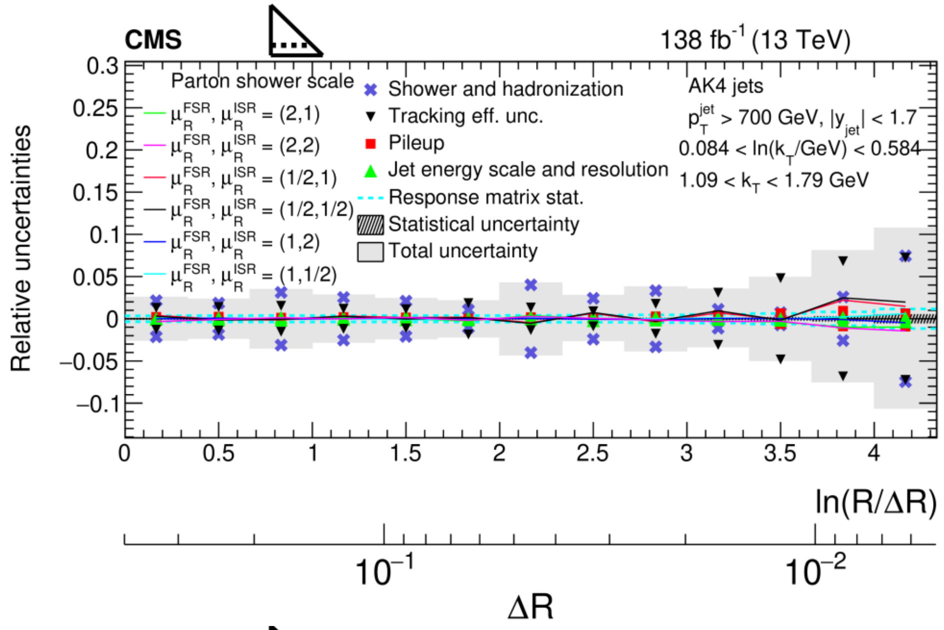

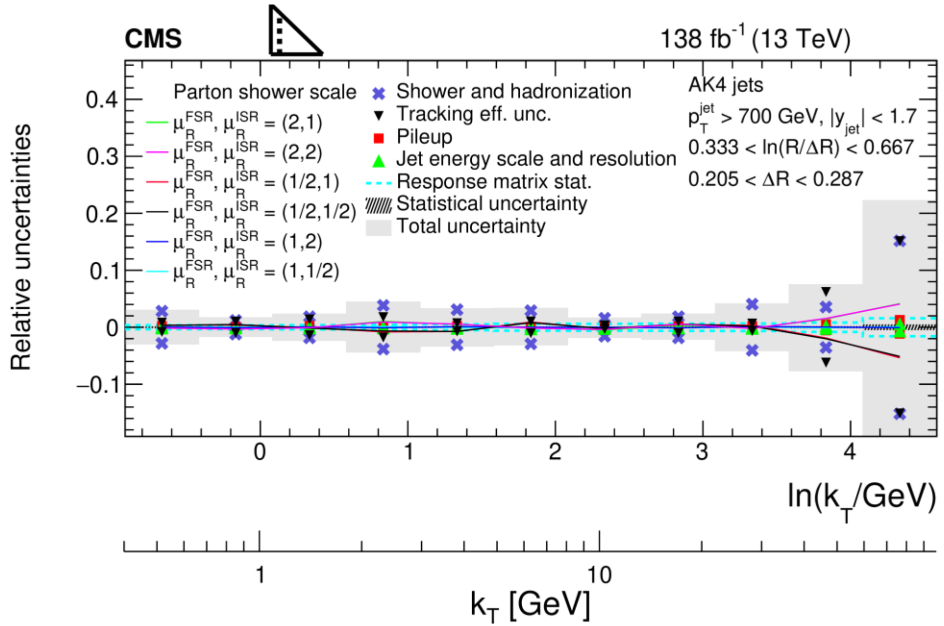

LJP: Constraining α_S^{FSR}

JHEP 05 (2024) 116

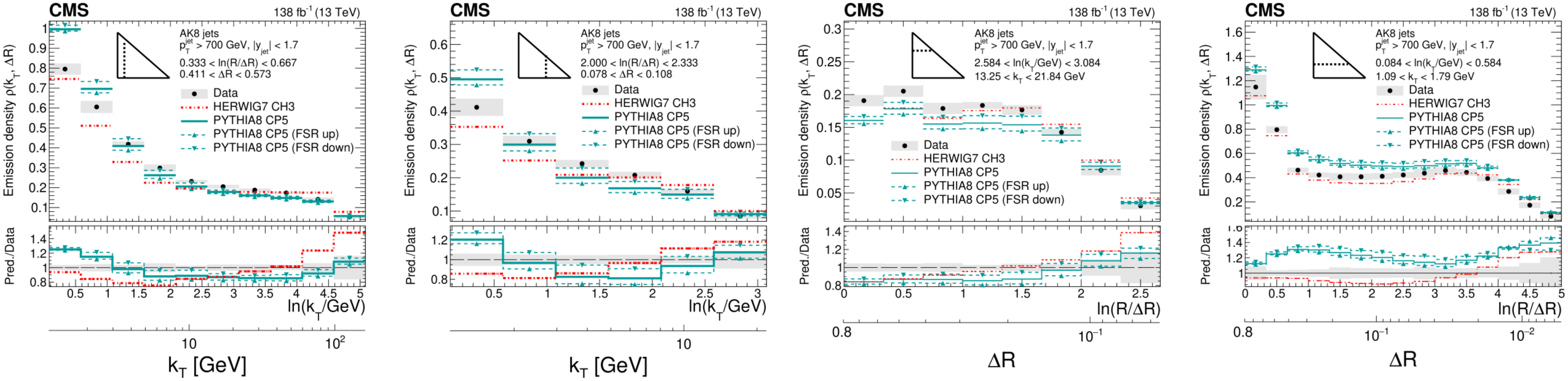

- Comparison of PYTHIA8 CP5 and HERWIG7 CH3 to data:

  → differences: PYTHIA8 CP5 15–20%, HERWIG7 CH3 5–10%

  neither describe data well in every region of the LJP

  → shapes of distributions similar for AK8 and AK4 jets

- LJP density linearly dependent on $\alpha_S^{\mathrm{FSR}}(m_Z)$:

  → sensitive to choice of renormalization scale

  → **~10% band** in perturbative region, shrinks at low k_T

  higher $\alpha_S^{\mathrm{FSR}}(m_Z)$ (FSR down) preferred at higher k_T

Missing NLO corrections in QCD branchings more relevant at high p_T where the shower evolves for longer

LJP: Constraining α_S^{FSR} (AK4)

JHEP 05 (2024) 116

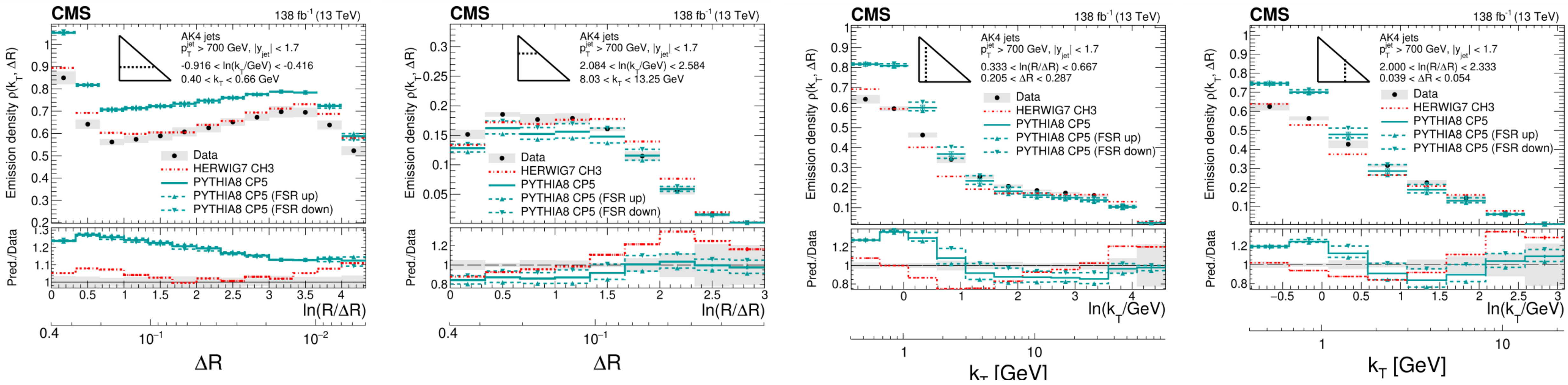

- Comparison of PYTHIA8 CP5 and HERWIG7 CH3 to data:

  → differences in bulk: PYTHIA8 CP5 15–20%, HERWIG7 CH3 5–10%

  neither describe data well in every region of the LJP

  → shapes of distributions similar for AK4 and AK8 jets

- LJP density linearly dependent on $\alpha_S^{\mathrm{FSR}}(m_Z)$:

  → sensitive to choice of renormalization scale

  → **~10% band** in perturbative region, shrinks at low k_T

  higher $\alpha_S^{\mathrm{FSR}}(m_Z)$ (FSR down)

Missing NLO corrections in QCD branchings more relevant at high p_T where the shower evolves for longer

LJP: PS models and UE tunes at low k_T

JHEP 05 (2024) 116

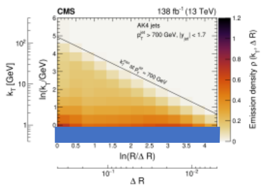

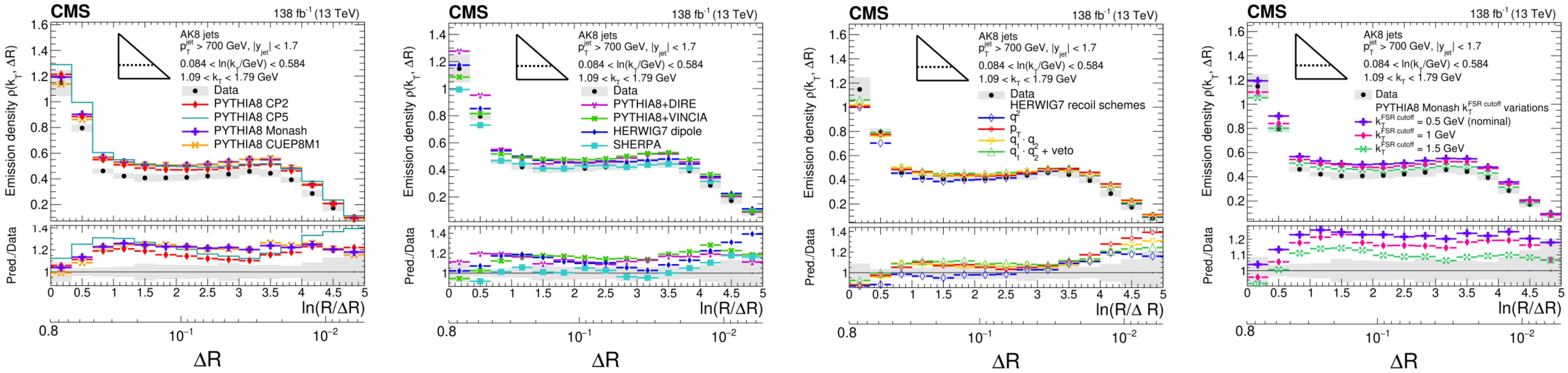

- At low k_T (dominated by hadronization and MPI contributions):
  - → PYTHIA8 **tunes:** higher values of $\alpha_S^{\mathrm{FSR}}(m_Z)$ preferred, less so than in bulk
  - → **dipole shower models:** HERWIG7, SHERPA **(cluster fragmentation)** in better agreement than **PYTHIA (Lund string fragmentation)**
  - → **angle-ordered Herwig7.2 recoil schemes:** q^2 best in non-pert. region
  - → **variations of** k_T **cutoff in** Monash tune: **larger** k_T^{FSR} **preferred**

- PYTHIA **consistently overshoots data** at low k_T irrespective of showering variations, renormalization scale choices (see backups)

- Generally, larger k_T^{FSR} to terminate FSR evolution more compatible with data across MCs (e.g., HERWIG7 and SHERPA $k_T^{\mathrm{FSR}} = 1$ GeV)

LJP: ATLAS & ALICE measurements

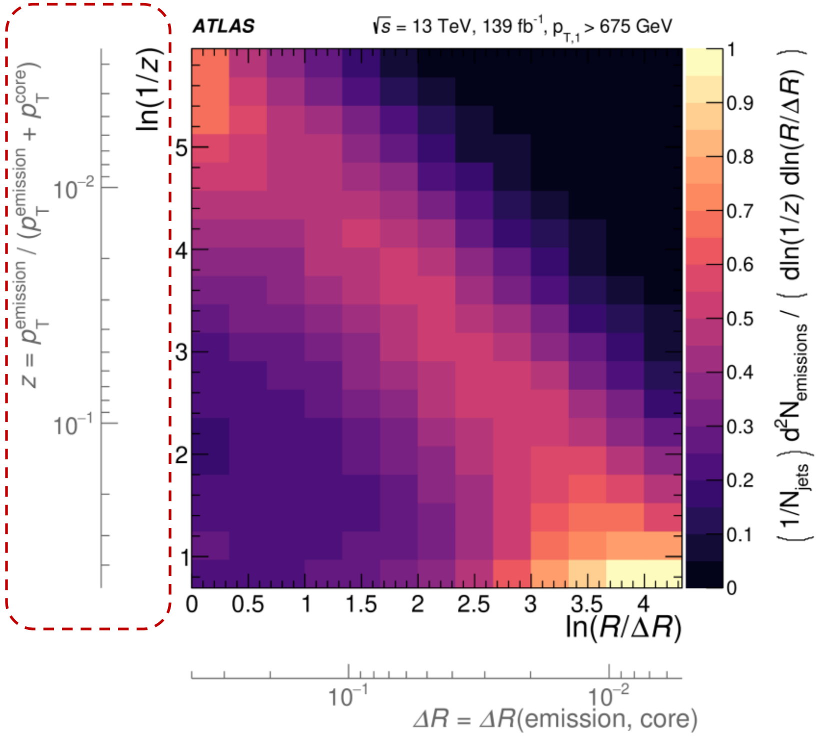

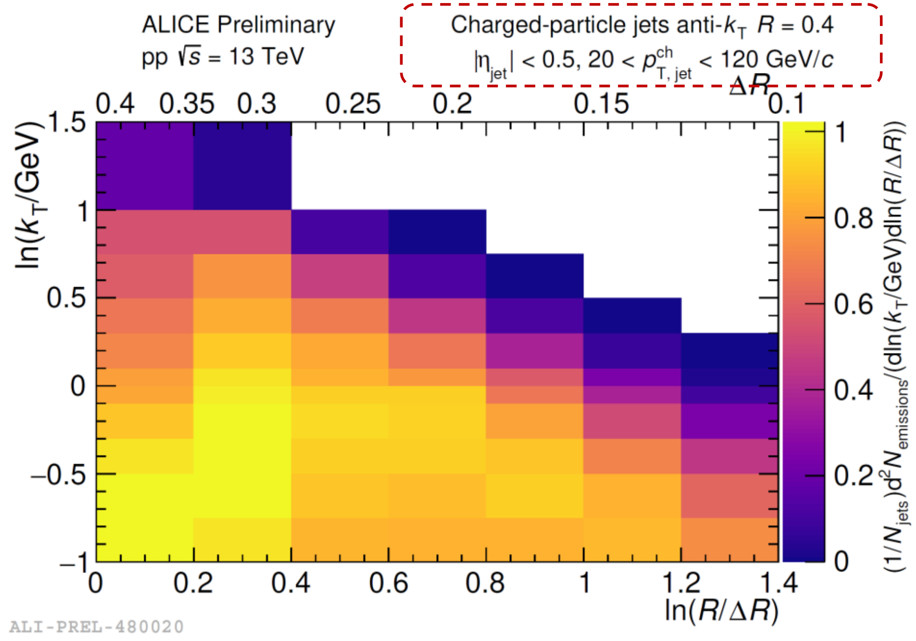

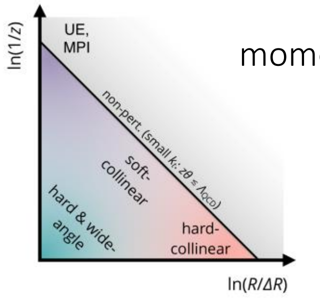

Different representation to CMS measurement, using momentum fraction $\ln(1/z)$ of emissions instead of k_T:

$$z = \frac{p_{T,softer}}{p_{T,softer} + p_{T,harder}}$$

Different range of measurement, $20 < p_{T,jet} < 120$ GeV; probing mostly the wide-angle region, using low- k_T splittings in small radius (R=0.4) jets,

EnCs: Unfolding and corrections

CERN-EP-2024-010

- Migration matrix for unfolding requires geometric matching of detector- and generator-level jets ($\Delta R < 0.2$) and (PF) particles
  - $\rightarrow$ uniquely matched at detector- and truth-level descriptions in nominal MC (PYTHIA8 CP5); mutually closest in plane of $\eta - \phi, \forall\ \Delta R(\triangle,\blacktriangledown) < 0.05$
  - $\rightarrow$ jet matching efficiency: $> 99\%$
  - $\rightarrow$ **purity correction (bin-by-bin fake subtraction) for** unmatched MC detector-level particles

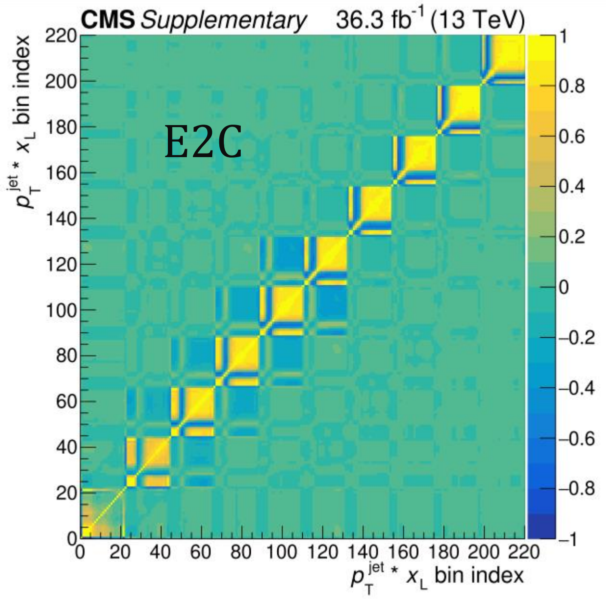

- Measurements unfolded multidimensionally in $\left(p_{T,\text{jet}}, x_L, \overbrace{\frac{\prod_{a=1}^{N} E_{i_a}}{E^N}}^{\text{energy weight}}\right)$ $[(8+2)\cdot(20+2)\cdot 20$ bins$]$
  - $\rightarrow$ multi-count observables, and two leading jets in event used $\Rightarrow$ large (upto 40%) statistical correlations between x_L and p_T bins, track both in input covariance matrices
  - $\rightarrow$ halve data being unfolded for EnC's, statistically decorrelated E2C and E3C unfolding
  - $\rightarrow$ iterative Bayesian unfolding (D'Agostini): 7 iterations until p-value > 0.05
  - $\rightarrow$ **efficiency (bin-by-bin)** correction for counts of unmatched particle-level objects

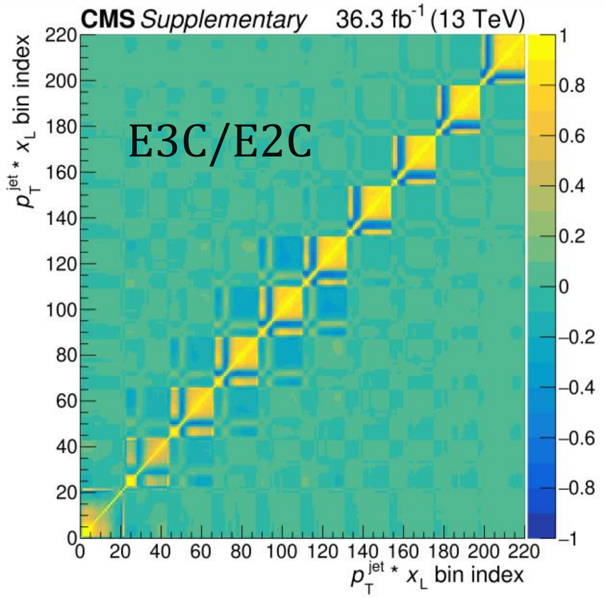

E2C: Unfolded measurements & uncertainties

[CERN-EP-2024-010]

- Data are compared to various parton shower models,
  - $\rightarrow$ no one model to describe them all (across p_T bins)
  - $\rightarrow \sim 10-15\%$ disagreement generally, similar to the primary LJP density measurement
- **Leading contributions** to uncertainties:
  - $\rightarrow$ shower and model uncertainties: $2-10\%$
  - $\rightarrow$ neutral hadron energy scale: $1-2\%$
- **Systematic** contributions considered:
  - $\rightarrow$ photon and charged/neutral hadron energy scale
  - $\rightarrow$ (global) jet energy scale and resolution
  - $\rightarrow$ PU, tracking efficiency, trigger prefiring
  - $\rightarrow$ QCD scale in parton shower and in hard scattering
  - $\rightarrow$ Underlying event tune, parton shower tunes
  - $\rightarrow$ PDF variations

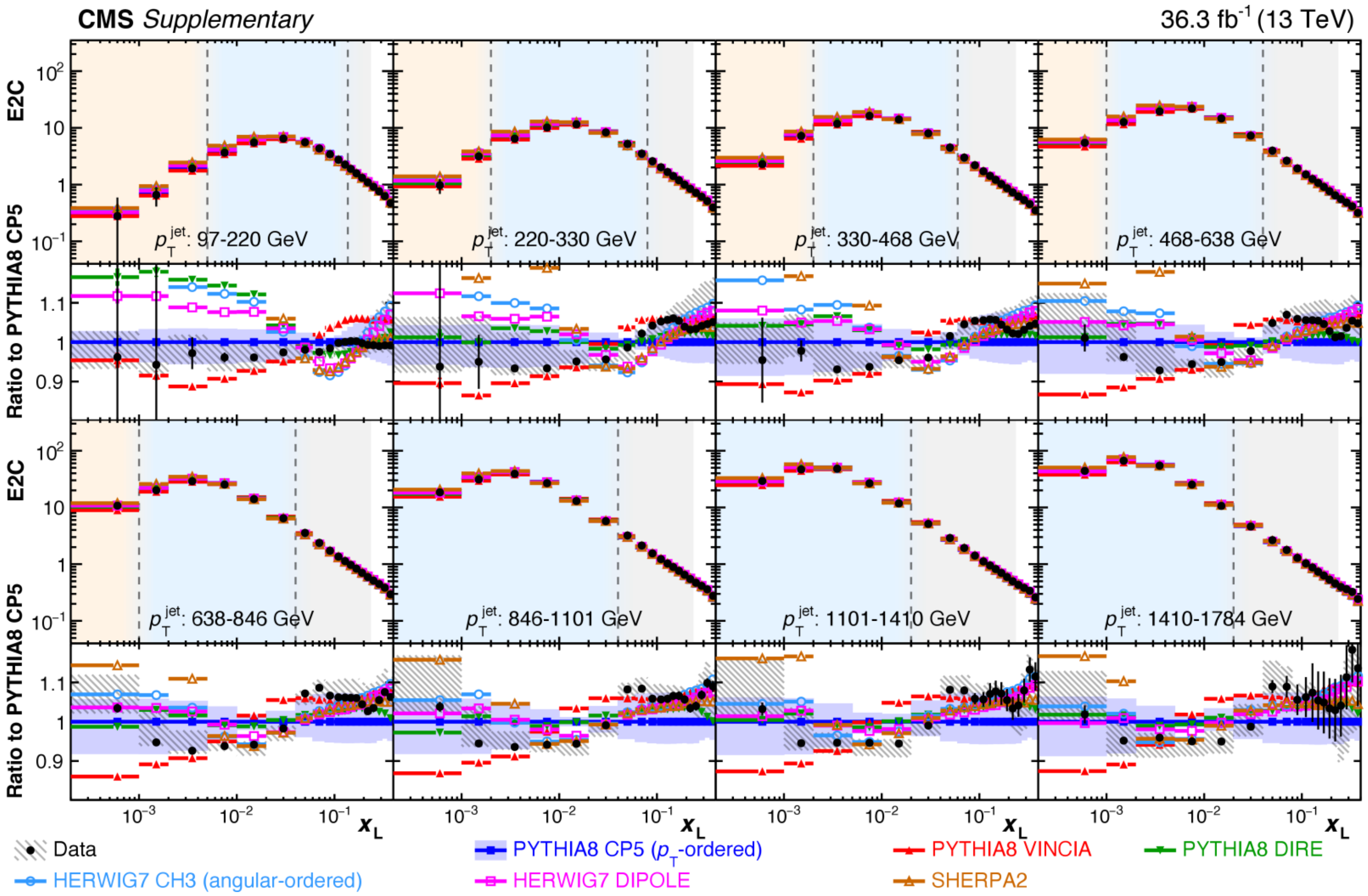

E3C: Unfolded measurements

CERN-EP-2024-010

$Q \propto x_L \cdot p_{T,\text{jet}}$: Boundaries between regions shift to smaller x_L at high p_T

- No one model to describe them all (across p_T bins)

  → $\sim 10-20\%$ disagreement generally, similar to the primary LJP measurement

- **Leading contributions** to uncertainties:

  → shower and model uncertainties: $2-10\%$

  → neutral particle energy scale: $1-2\%$

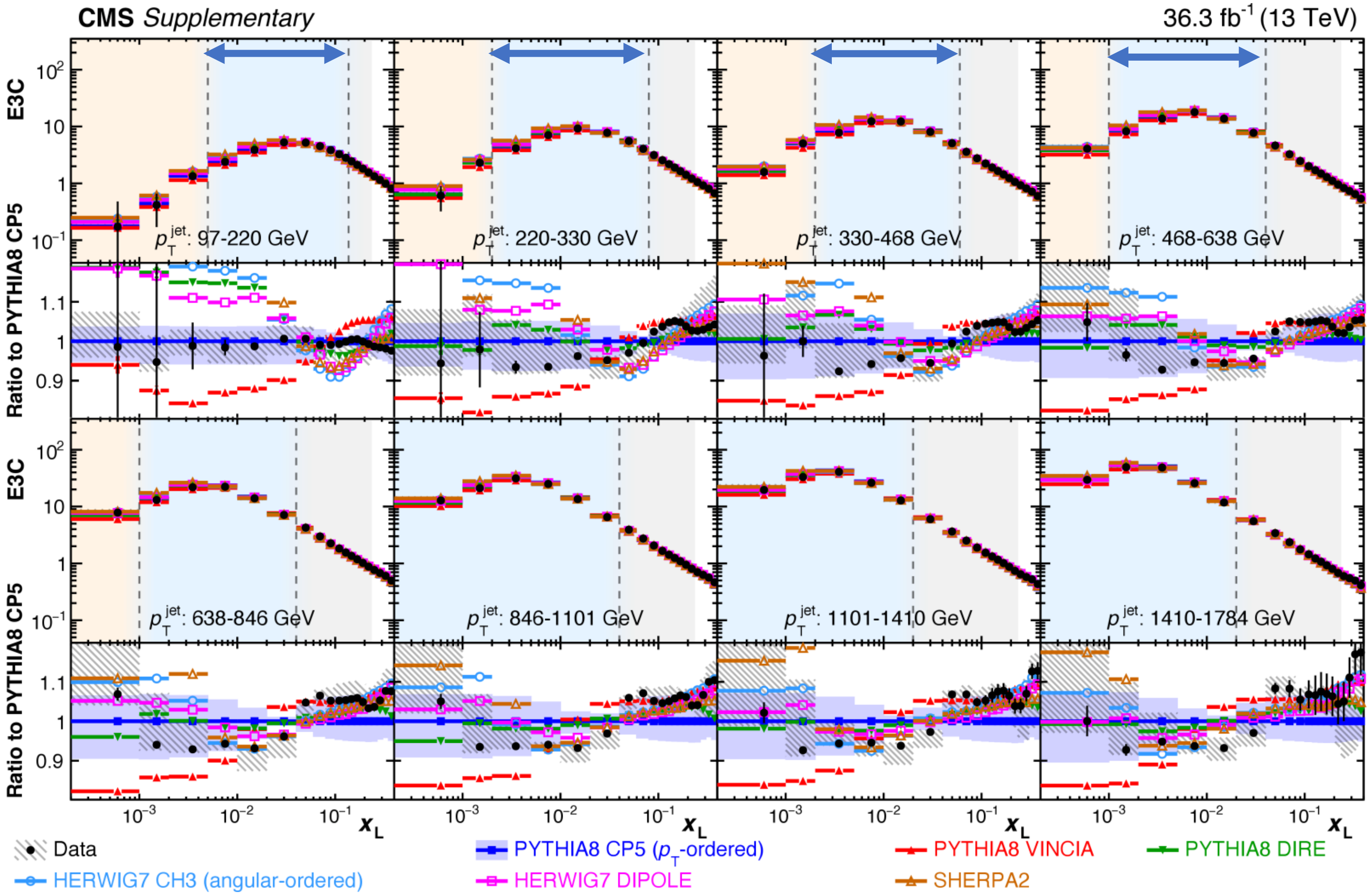

$$x_L \simeq \frac{0.8}{p_{T,\text{jet}}} \longleftrightarrow x_L \simeq \frac{20}{p_{T,\text{jet}}}$$

E3C/E2C: Comparisons to NLO+NNLL$_{approx}$

CERN-EP-2024-010

W. Chen, J. Gao, Y. Li, Z. Xu, X. Zhang, HX. Zhu; JHEP 05 (2024) 043

- Bin-by-bin **hadronization factor** applied to NLO+ NNLL$_{approx}$ calculations to match to unfolded hadron-level measurement

  → account for $p_T > 1$ GeV threshold for hadrons, averaged **hadron/parton level** distributions in PYTHIA and HERWIG

  → corrections 5-40% for E2C, E3C and 0-3% in ratio

- Data shapes agree well with calculations

- Theory systematics

  → QCD scale of NNLL$_{approx}$ predictions and of hard scattering

  → hadronisation factors, UE/PS modeling, PDF uncertainties

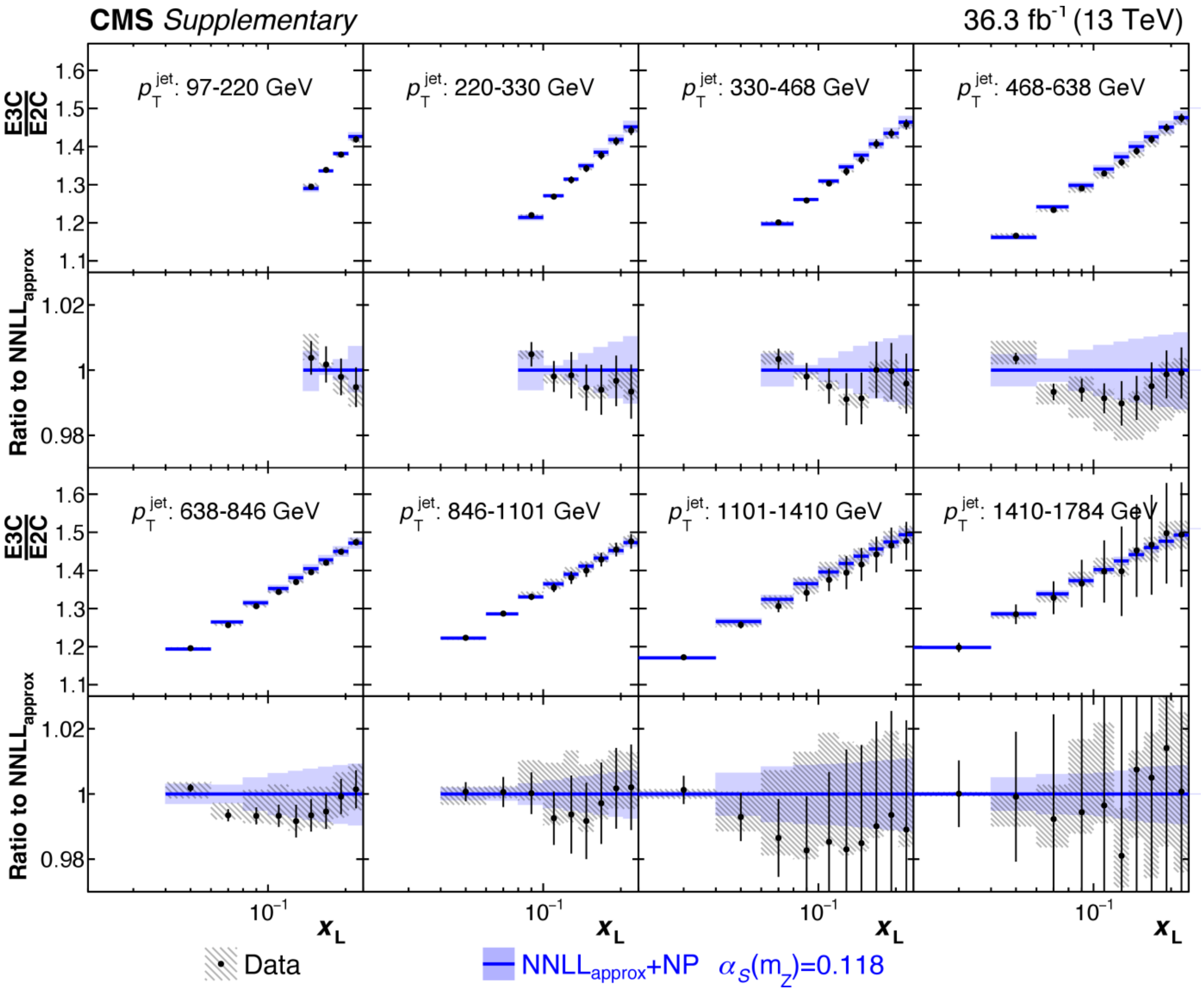

D'Agostini unfolding

- Iterative, unfolding with a stopping criterion over steps t, number of iterations $\leftrightarrow$ level of regularisation

$$\lambda_j^{(t+1)} = \lambda_j^{(t)} \sum_{i=1}^{n} \frac{R_{i,j} v_{obs,i}}{\sum_{k=1}^{n} R_{i,k} \lambda_k^{(t)}}$$; input prior (MC): $\lambda^{(0)} = \lambda^{MC} \left(v_{obs,\,\mathrm{MC}}\right)$

- χ^2-test in smeared space:

  $\rightarrow$ test compatibility of unfolded particle-level distribution, folded back to detector level

  minimize: $$\chi^2 = \left(\vec{v}_{observed} - \vec{v}_{folded}\right) V^{-1}_{(\mathrm{stat.\ only})} \left(\vec{v}_{observed} - \vec{v}_{folded}\right)$$

  $\rightarrow$ stop when folded and input (data-bkg.) distributions are statistically compatible ($p > 0.05$)

- **LJP measurement:** Decorrelating shower and hadronization uncertainties by uncorrelated variations of response matrix and input prior from nominal and alternate MCs: PYTHIA8 CP5 and HERWIG7 CH3; take the difference between unfoldings with nominal RM+MC prior (PYTHIA8+PYTHIA8) and alternates: (PYTHIA8+ HERWIG7), (HERWIG7 +PYTHIA8)

  $\rightarrow$ estimate **uncorrelated** systematic from symmetrized variations of shifts of alternate unfoldings